ABSTRACT

Title of Thesis: FREE-SPACE OPTICAL COMMUNICAITONS THROUGH A FOREST CANOPY

Clinton Lee Edwards, Master of Science, 2004

Thesis Directed By: Professor Christopher C. Davis, Department of Electrical and Computer Engineering

This paper models the effects of the leaves of mature broadleaf trees on air-to-ground free-space optical (FSO) communication systems operating through the leaf canopy. Ecological radiation transfer models are considered and the concept of Leaf Area Index (LAI) is reviewed and related to a probabilistic model. Leaf transmittance is experimentally measured for different leaf types and determined to be very close to zero. A probabilistic canopy model of foliage is developed as obscuring leaves are randomly distributed throughout the treetops. The expected fractional unobscured area statistic is derived as well as the variance around the expected value. Monte Carlo simulation results confirm the probabilistic model's statistical conclusions. Multi-site passive optical measurements are taken in a mature broadleaf forest environment with increasing leaf obscuration then fitted to the model. The model's implications to FSO system links are considered and simulated. Conclusions are discussed as well as further research.

FREE-SPACE OPTICAL COMMUNICAITONS THROUGH A FOREST CANOPY

by

Clinton Lee Edwards

Thesis submitted to the Faculty of the Graduate School of the
University of Maryland, College Park, in partial fulfillment
of the requirements for the degree of
Master of Science
2004

Advisory Committee:
Professor Christopher C. Davis, Chair
Professor William S. Levine
Professor Thomas E. Murphy

Dedication

I would like to dedicate this work to my wife, Corinne. She has supported my desire to further my education despite the abject poverty that is associated with being a graduate student. Only with her unflinching love and support, this work has been completed. I also dedicate this to my children, Sheely and Xavier, who have tolerated my absences from the dinner table to complete this work as well. Finally, I would like to dedicate this to my parents, M. Lee Edwards and Patricia H. Edwards.

Acknowledgements

This is certainly not the result of my efforts only. There are many people to whom I owe a great debt of gratitude for giving encouragement and inspiration throughout this project. First, I must thank my advisor, Dr. Chris Davis, for functioning as a sounding board for ideas and helping this project take shape. Dr. Davis has also provided the funding for this work. I want to thank Dr. William Levine for helping with the random processes and probability issues that are contained in this paper. Also I would like to thank Dr. Thomas Murphy for agreeing to serve on my thesis committee.

I would like to acknowledge Dr. Robert Gammon and Mr. Allen Monroe for the use of the Physics Graduate Laboratory resources to experimentally measure foliage transmittance. PhD Candidate Jon Alder of The Johns Hopkins University was instrumental in assisting with the passive optical canopy imaging and measurements. My officemates, Jaime Llorca, Shawn Ho, and Sugi Trisno have been invaluable in developing many of these ideas.

Table of Contents

List of Tables

List of Figures

Chapter 1: Introduction

1.1 Free-Space Optical Communications

Today optical fiber carries terabits-per-second to a vast host of users who are interested in information in the form of voice, fax , video, documents, and web pages. While optical fiber represents the upper limit of available bandwidth and high data transfer rates it also requires time to install the optical cables.

Free-space optical (FSO) communication technology can provide high data rate transfer and can be easily installed, moved or reconfigured as needs change. FSO technologies are intrinsically secure because of the line-of-sight requirement as well as the high directivity of the optical beam. Both of these features create a low probability of intercept (LPI) for the user's data.

Search and Rescue personnel have for a long time used optical beacons to locate or communicate through hazardous conditions with others. The military concept of "total battlefield connectivity" has furthered the need for accurate modeling of the dynamic channel that can affect the FSO system performance.

1. 2 Need for FSO Foliage Model

Some obscuring elements in the communication channel include: dust, smoke, fog, foliage, turbulence, wind and birds [3, 10]. Though much work has been done to optimize the communication hardware and software for FSO links [22], a literature search has revealed no previous investigations in foliage modeling for FSO communication links.

Motivated by an air-to-ground communication scenario between a receiver and aerial vehicle, possibly an unmanned aerial vehicle (UAV), we set out to investigate and model the obscuration of FSO communications by broadleaf mature forest foliage. The objective of this project is to develop a probabilistic model for air-to-ground FSO applications that characterizes the obscuration due to the foliage.

The model must be quantitative, so that it can be applied to FSO systems and used to predict system performance. The model must be consistent with radiation models that ecologists use to model photosynthetic effects and the health of a forest. Finally, the probabilistic model must allow for system operational geometry variation such as different laser light angles as it penetrates the canopy, leaf sizes or canopy thickness.

1.3 Chapter Summaries

Chapter 2 consists of a discussion of the link equation that must be considered for all FSO systems. System components are considered such as transmitted power, beam

focusing or optical gain, channel loss or Link Loss due to obscuration or turbulence and receiver characteristics such as aperture.

Chapter 3 discusses other research efforts to characterize foliage. Ecological transfer models will be reviewed and the concept of leaf area index (LAI) will be discussed as it relates to Beer's Law. Two NASA efforts to analyze the vertical leaf distribution of treetops using LIDAR and LADAR technologies are covered. The assumption of the treetop "canopy" will be motivated by ecological and NASA literature.

Chapter 4 contains the development of our probabilistic model. Leaves are randomly placed in the canopy. The canopy is broken into cells whose size is relative to the average size of the leaves in the canopy. Leaf placement is uniform and independent of other cells and previous leaf placements in the canopy or is independent and identically distributed (IID). The probability of a single cell remaining unobscured is analyzed and then extended to a region of cells in the canopy through a binomial distribution. An average fractional unobscured area statistic is developed as well as the variance around the average for the canopy. A Monte Carlo simulation with Matlab confirms the probabilistic model development.

Chapter 5 consists of experimental measurements conducted with a passive optical device and supporting apparatus. Experimental apparatus design is discussed as well as the technique for recording the best measurements. The probabilistic canopy model is fitted to the measurements and also confirms model assumptions. The

ecological model is related to the probabilistic canopy model and physical meaning of variables in the canopy model is discussed.

Chapter 6 applies the new model for mature broadleaf canopies and looks at its implication for FSO communication systems. Leaf obscuration is folded into the "Link Loss" term of the link equation for a FSO system. Leaf size and aperture size as well as the leaf area index (LAI) affect over-all system performance. Simulations are performed using new canopy probability model and analyze the signal-to-noise ratio (SNR) of a UAV approaching a receiver from several kilometers away. The SNR is greatest when the UAV is directly above the ground receiver or transmitter and the ratio of receiver aperture to average leaf size is as large as possible.

Chapter 7 consists of conclusions for this project as well as future work. Both measurements and Monte Carlo simulations closely support the probabilistic canopy model. Future efforts are described including investigation of the effects of wind on the forest canopy, different leaf distributions, and multi-scatter scenarios. Actual FSO communication system measurements are considered for an aerial vehicle.

Chapter 2: FSO Link Equation

2.1 Link Equation

For a FSO communication system the "Link Equation" relates the power transmitted to the power received. For ideal channels, the power received is the power transmitted. However, most systems are not close to ideal and the link equation must be developed so the designer can determine critical parameters such as transmitter power, received power and implementation losses.

Figure 2.1 illustrates a FSO system that is obscured by foliage and includes parameters as transmitter power, receiver aperture area, optical gain or focusing factor, and *Link Loss* that occur in the channel between the transmitter and receiver. Other channel losses not considered in the diagram may include imperfections in optical components, beam alignment, beam coupling in optical elements in receivers or transmitters.

Link equations are generally fed into a noise model that accounts for different sources of noise such as quantum and thermal noise. The link equation and noise model are used to carry out the bit-error calculation that takes into consideration the modulation technique. The bit-error calculation outputs the bit-error-rate (BER) and provides a

benchmark of reliability for the overall FSO system. Figure 2.2 illustrates the FSO link equation relating transmitted and received power.

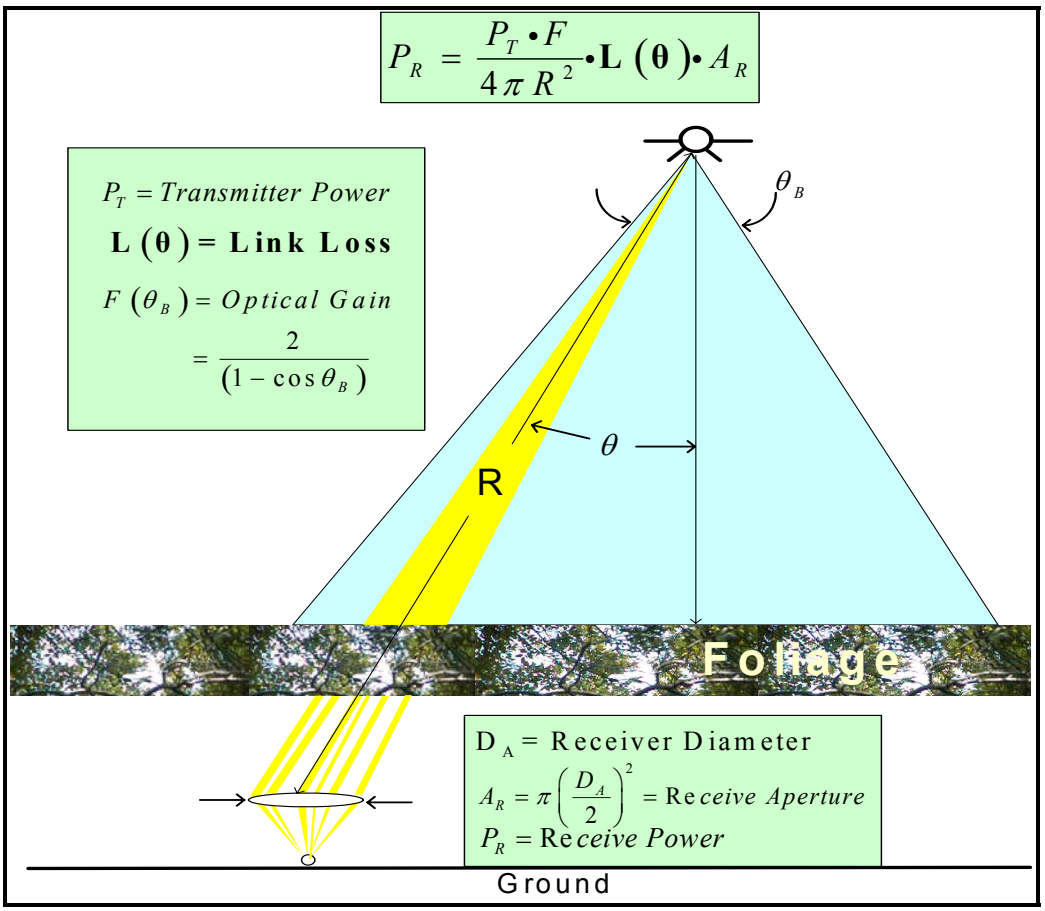

Figure 2.1 Development of the "link equation" for air-to-ground communication with partially obscuring foliage.

2.2 Focusing Factor

The focusing factor or antenna gain is a measure of a transmitter's ability to focus the electromagnetic field into an area at a distance R compared to an isotropic radiator. For a beam with beam divergence θ_B, the focus factor is simply:

$$F(\theta_B) = \text{Focusing Factor}$$

$$= \frac{\dfrac{1}{\iint\limits_{\varphi=[0,2\pi]\ \theta=[0,\theta_B]} R^2 \sin(\theta)\, d\theta d\varphi}}{\dfrac{1}{4\pi R^2}}$$

$$= \frac{4\pi R^2}{2\pi R^2 \int\limits_{\theta=0}^{\theta=\theta_B} \sin(\theta)\, d\theta}$$

$$= \frac{2}{\left[1-\cos(\theta_B)\right]}$$

Theoretically, $F(\theta)$ *ranges from one to positive infinity* $\left(F(\theta):[1,\infty]\right)$***;*** but, practically, an upper limit exists.

2.3 Link Loss

Link Loss is affected by all parameters between receiver and transmitter or "the channel" that would cause electromagnetic energy to not reach the receiver. It may include turbulence, fog, smoke, dust, foliage, and birds. The link loss ranges between zero and one $\left(L(\theta)=[0,1]\right)$ and is the fraction of power that reaches the receiver. The link loss combined with the power transmitted and the focus factor yield the entire ingredients to determine the power density at the receiver.

As in Figure 2.2, if power density at the receiver is measured in units of power per area, then received power is calculated by multiplying the power density by the area of the receiver aperture.

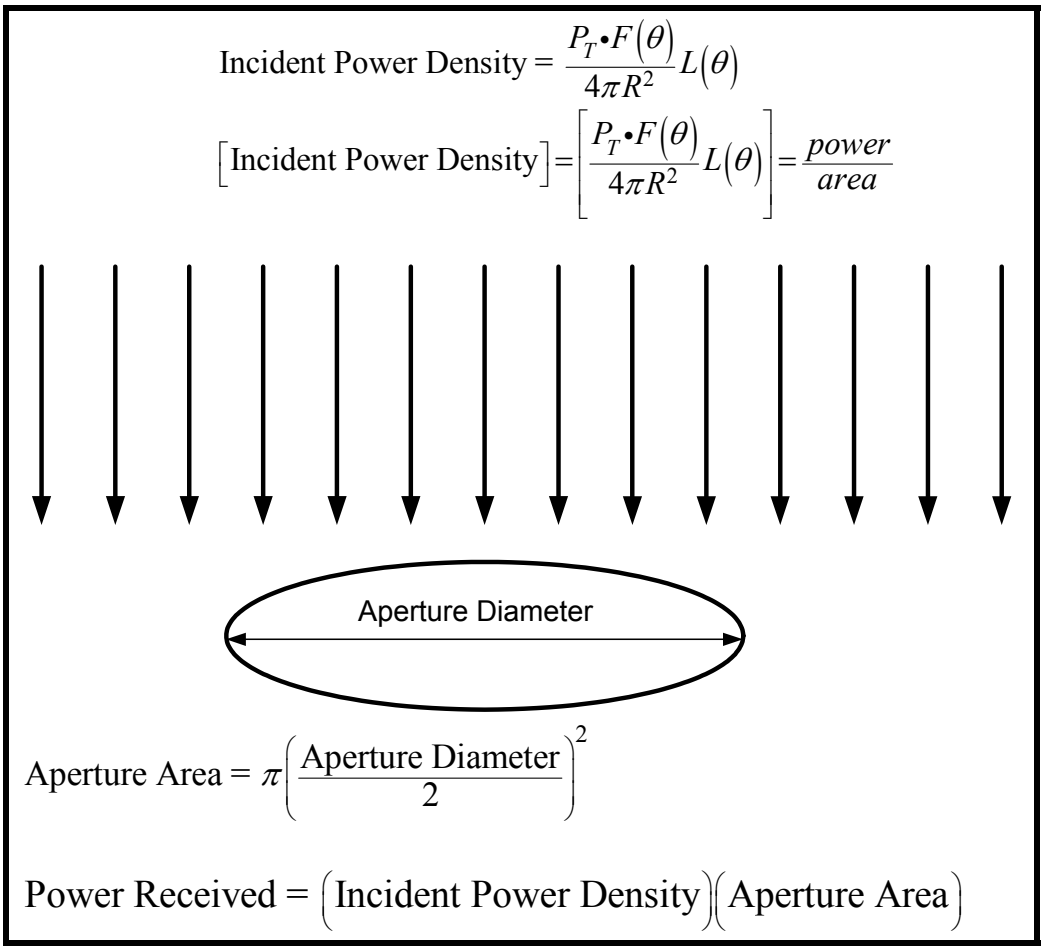

Figure 2.2 Incident power density on an aperture.

Chapter 3: Ecological Model and NASA Measurements

3.1 Ecological Model

For decades forest foliage has been of interest to ecologists who have investigated forest composition, and environmental resource managers, who analyze forest productivity and stages of its life cycle. This is especially important for endangered species of trees. Many Ecologists are interested in the photosynthesis that occurs as light and leaves interact, as well as biomass, leaf area index (LAI), tree height, and other statistics that define the structure of a forest [6]. Leaf cover densities as well as reflections from the foliage at different wavelengths are indicators of the health and age of a forest [20].

Young forests have foliage concentrated near ground level while "mature forests," generally over 75 years old, have a canopy of foliage well above the ground. The third classification is the "old growth" forest that is a combination of mature and young trees and foliage distributed throughout the vertical dimension.

3.2 Beer's Law and LAI

Theoretical analysis of the radiation transfer model through foliage has grown from an extension of Beer's Law, which characterizes radiation passing through a medium (liquid or gas) containing a concentration of absorbers [5,7]. Depending on the path

length, z, and concentration, γ, of the absorbing material in the solution, the exiting radiation intensity is reduced exponentially. The left side of Figure 3.1 depicts photons entering a beaker and the reduced amount exiting the beaker. Ecologists have extended this model to a macroscopic foliage environment. In this extension, leaves take the place of absorbing material and the entering intensity of light is related to the exiting intensity by two parameters: the Leaf Area Index (LAI) and the constant *k* that describes the geometric distribution and optical properties of the leaves [19]. If the leaves are opaque and multi-scattering does not occur then *k*=1.

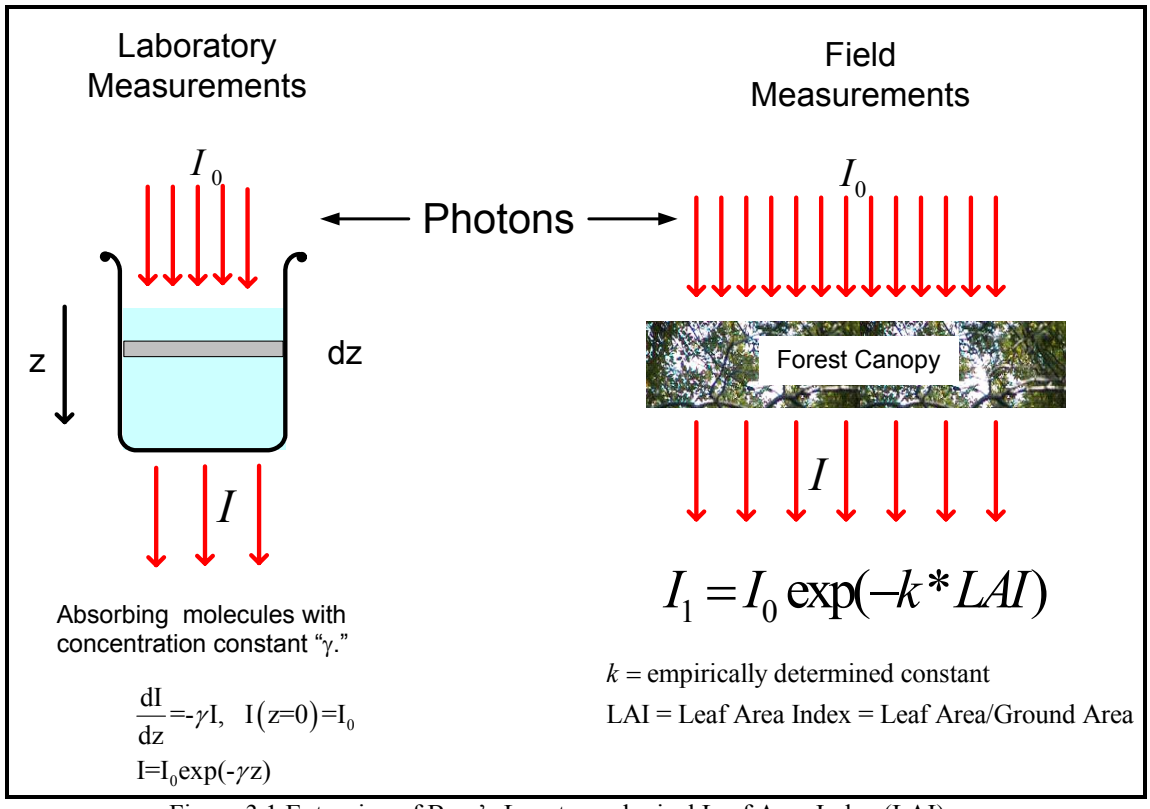

Figure 3.1 Extension of Beer's Law to ecological Leaf Area Index (LAI)

Leaf Area Index, physically, represents a ratio of the sum of one-sided leaf area projection in a region to the ground area in the same region. Ecologists use the concept of LAI to determine the percentage of light that will penetrate the canopy. The interest in the LAI statistics is driven by their correlation to photosynthesis properties in forested areas. Figure 3.2 displays several different LAI.

A review of the literature has not yielded an analytic proof supporting this leap from the microscopic to the macroscopic regime. However this paper will, in due course, present a probabilistic approach that supports this extension.

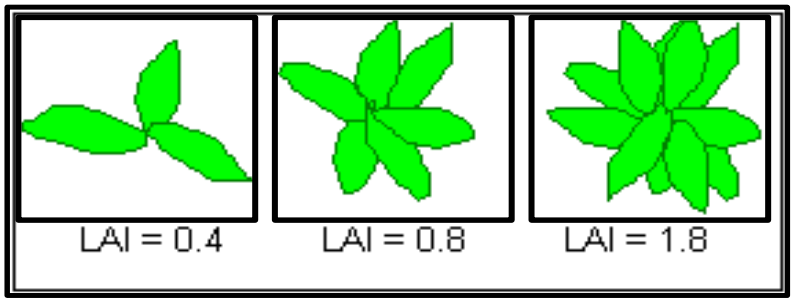

Figure 3.2 Examples of Leaf Area Index (LAI) values

3.3 Remote Sensing Measurements

One technology to quantify or measure LAI is the use of LIDAR systems. Unlike other optical sensors and longer wavelength devices, LIDAR is capable of measuring the distribution of the foliage in the vertical direction [16]. Longer wavelengths, like microwaves, tend to penetrate the foliage. Other optical sensors, while utilizing spectral diversity and the electromagnetic properties of forest elements, still cannot

give detailed information about moderate and high biomass forests. Thus, LIDAR instruments are preferred to provide detailed information about forest composition, either on airborne or space platforms. By sending out well-defined pulses of light and then sensing the reflected backscatter signal as a function of accurate and precise time, the distance between the sensor and target is determined [12, 15]. Figure 3.3 is an artist's rendition of the LIDAR footprint reflecting off a treetop (picture courtesy of NASA Goddard Space Flight Center, NGSFC).

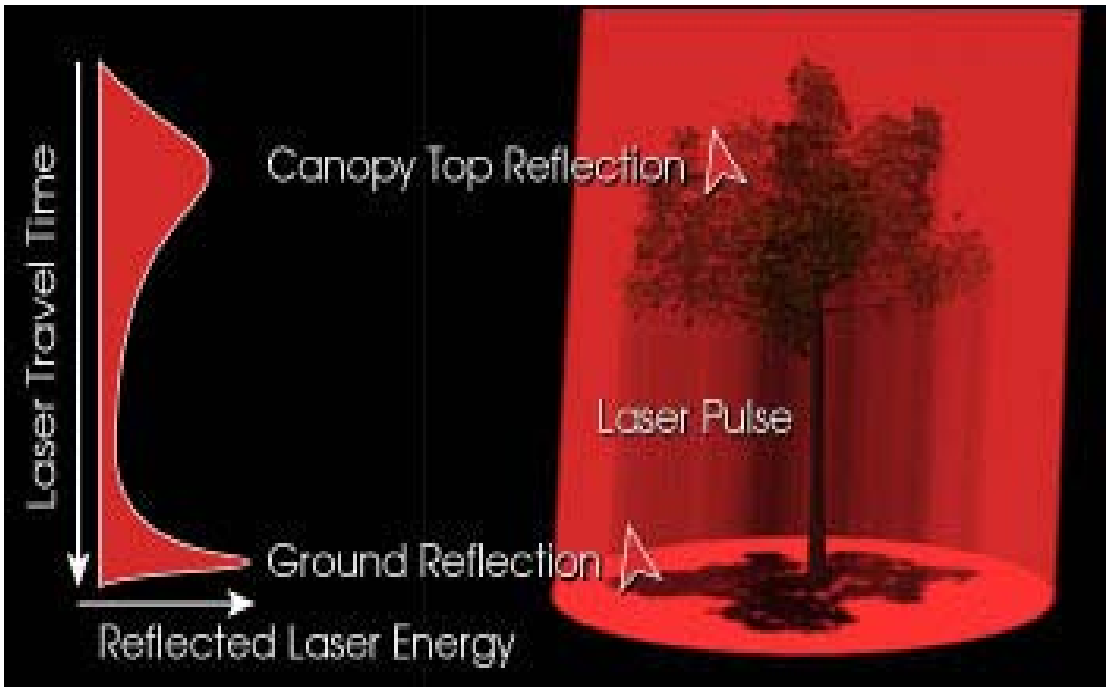

Figure 3.3 LIDAR used to determined the density and distribution of tree foliage.

SLICER (Scanning LIDAR Imager of Canopies by Echo Recovery) and VCL (Vegetation Canopy LIDAR) are two efforts to use laser altimetry remote sensing to characterize forest foliage [14, 15]. SLICER generates a digitized waveform that is proportional to the density of the canopy in the vertical direction. Figure 3.4 illustrates a LIDAR remote sensing system that is generating a vertical distribution of

foliage. SLICER operates in the near infrared at 1064nm and has a laser footprint of 5-25 meters.

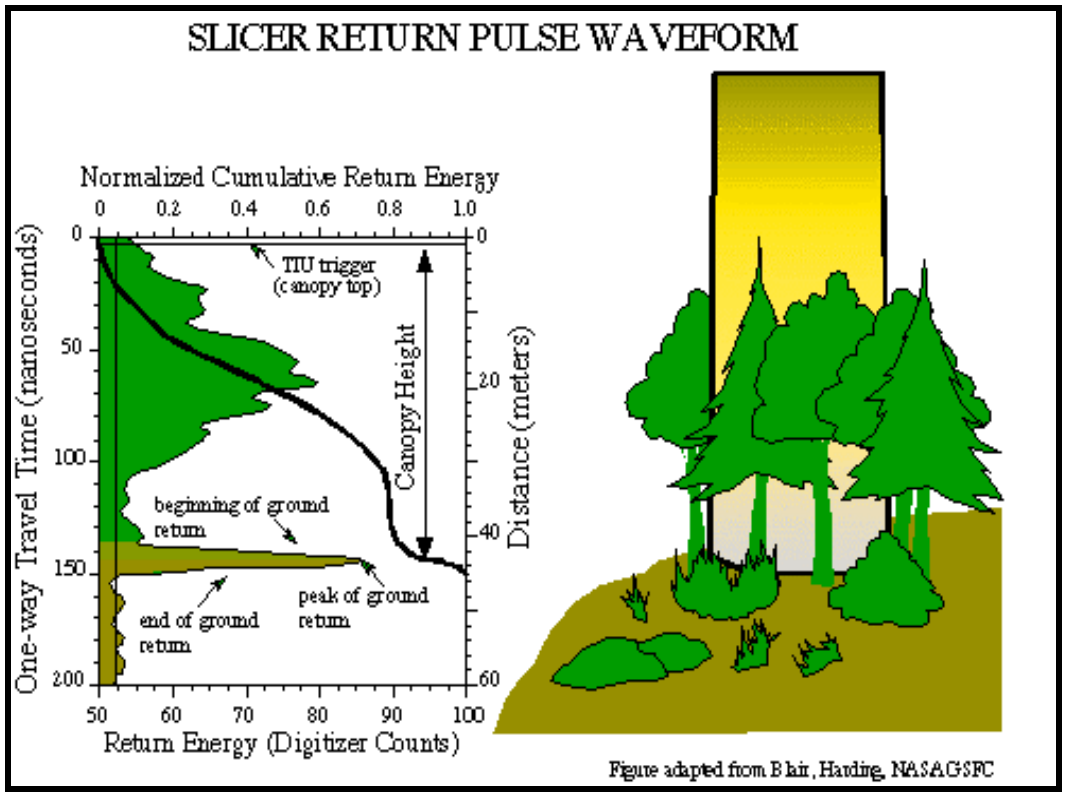

Figure 3.4 SLICER uses LIDAR to develop digitized waveform of foliage.

Chapter 4: Probabilistic Canopy Model

4.1 Specifications of Model

Motivated by the need to characterize the attenuation in penetrating optical intensity due to the leaves in a canopy, the following assumptions have been made for mature broadleaf forest foliage:

- Canopy region can be divided into cells that are related to leaf size.
- Placement (size and orientation) of leaves in mature forest is (uniformly) independent identically distributed (IID).
- Canopy structure exists with foliage concentrated well above the ground.
- Tree leaves are "broadleaf" such as maple, sweet gum, oak, etc.
- Leaf transmission is zero.

Figure 4.1 illustrates a region of the canopy, which can be divided into sections of n "cells" that are the average size of a leaf in the canopy. Assuming that the cells are the average size of a leaf in the canopy and that the placement of leaves is independent identically distributed (IID) [6], for n cells, the probability that placing a single leaf obscures any one cell is:

$$\Pr\left\{\text{a leaf is placed in i}^{\text{th}}\textit{cell}\right\} = \Pr\{\text{i}\}$$

$$\Pr\{\text{i}\} = \frac{1}{n}$$

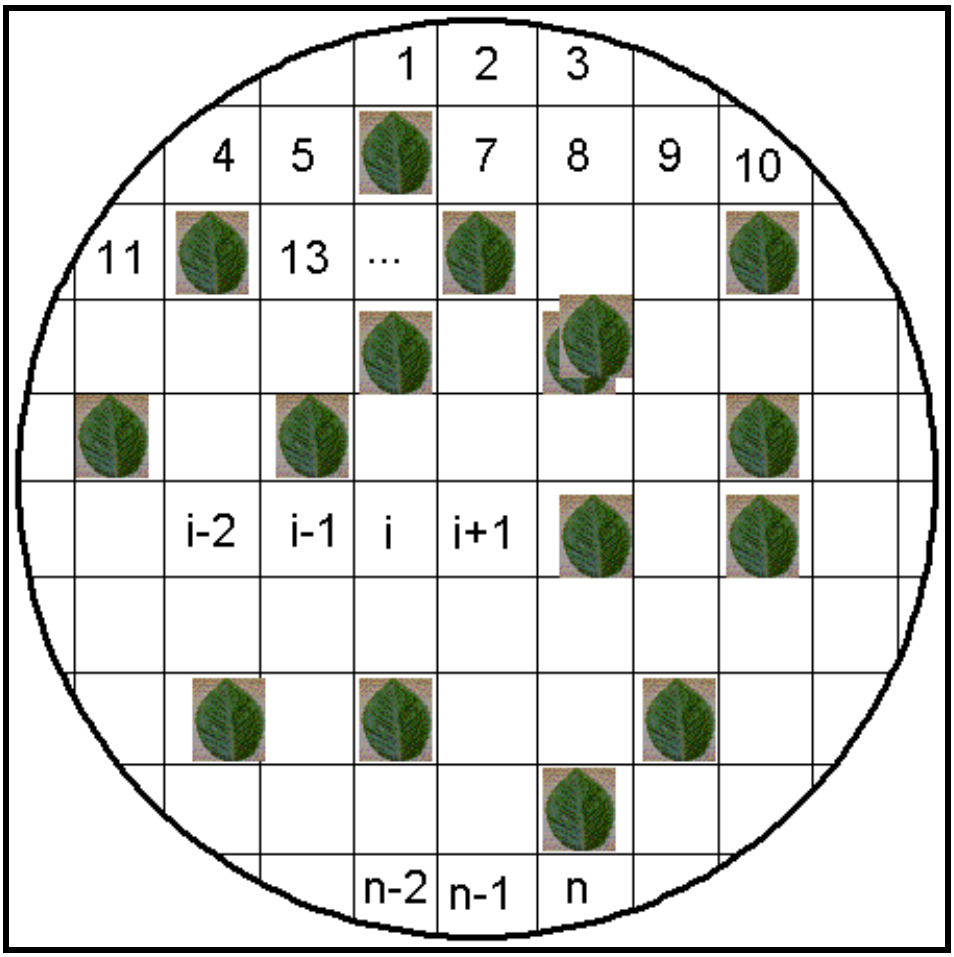

Figure 4.1 Canopy region divided into *n* cells as *m* leaves are uniformly distributed.

Because the distribution of leaves is independent and identically distributed, the probability that the ith and i+1 cells will contain a leaf after two leaves are randomly placed is:

$$\begin{aligned}\Pr\{i \cap i+1\} &= \Pr\{i\}\Pr\{i+1\} \\ &= \left(\frac{1}{n}\right)\left(\frac{1}{n}\right) \\ &= \left(\frac{1}{n}\right)^2\end{aligned}$$

By the same reasoning the probability that any single cell will have two leaves land in it after two leaf placements (one leaf on top of the other leaf) is:

$$\begin{aligned}\Pr\left\{2 \text{ leaves in the i}^{\text{th}} cell\right\} &= \Pr\{i\}\Pr\{i\} \\ &= \left(\frac{1}{n}\right)\left(\frac{1}{n}\right) \\ &= \left(\frac{1}{n}\right)^2\end{aligned}$$

Therefore for the probability of *m* specified events occurring in *m* leaf placements is:

$$\Pr\{\text{m leaves in specified cells}\} = \left(\frac{1}{n}\right)^m$$

Since we are interested in the unobscured space in the canopy, let's consider the complementary problem: Let X_i be the event that no leaf is in the i^{th} cell after a single leaf is placed:

$$\Pr\{X_i \mid 1 \text{ leaf placed}\} = \left(1 - \frac{1}{n}\right)$$

Extending it to two leaves and because of the IID property, the probability of X_i is:

$$\Pr\{X_i \mid 2 \text{ leaf placed}\} = \left(1-\frac{1}{n}\right)\left(1-\frac{1}{n}\right)$$
$$= \left(1-\frac{1}{n}\right)^2$$

After m leaves have been placed, the probability of X_i is:

$$\Pr\{X_i \mid m \text{ leaf placed}\} = \left(1-\frac{1}{n}\right)^m$$

Though it is not readily obvious, for $n>>m$ or sufficiently large m leaves and n cells in the canopy:

$$P\{X_i\} = \left(1-\frac{1}{n}\right)^m$$
$$\left(1-\frac{1}{n}\right)^m \approx e^{\frac{-m}{n}}$$

The Taylor series about zero of the right hand term is:

$$e^{\frac{-m}{n}} = \sum_{j=0}^{\infty} \frac{\left(-m/n\right)^j}{j!} = 1-\frac{m}{n}+\frac{\left(m/n\right)^2}{2!}-\frac{\left(m/n\right)^3}{3!}+\frac{\left(m/n\right)^4}{4!}-\ldots$$

Expanding the left-hand term with the binomial distribution yields:

$$\left(1-\frac{1}{n}\right)^m = \sum_{k=0}^{m}\binom{m}{k}(1)^k\left(\frac{-1}{n}\right)^{m-k} = \sum_{k=0}^{m}\left(\frac{m!}{k!(m-k)!}\right)\left(\frac{-1}{n}\right)^{m-k}$$

Because the terms can be added in any order, the indices can be reversed:

$$\sum_{k=m}^{0}\left(\frac{m!}{k!(m-k)!}\right)\left(\frac{-1}{n}\right)^{m-k} = \left(\frac{m!}{m!(m-m)!}\right)\left(\frac{-1}{n}\right)^{0} + \left(\frac{m!}{(m-1)!(m-m+1)!}\right)\left(\frac{-1}{n}\right)^{1} + \left(\frac{m!}{(m-2)!(m-m+2)!}\right)\left(\frac{-1}{n}\right)^{2} + \ldots + \left(\frac{m!}{(m-m)!(m-m+m)!}\right)\left(\frac{-1}{n}\right)^{m}$$

Simplifying the terms yield:

$$\sum_{k=m}^{0}\left(\frac{m!}{k!(m-k)!}\right)\left(\frac{-1}{n}\right)^{m-k} = 1-\left(\frac{m}{n}\right)+\frac{m(m-1)}{(2!)n^2}-\frac{m(m-1)(m-2)}{(3!)n^3}+\frac{m(m-1)(m-2)(m-3)}{(4!)n^4}-\frac{m(m-1)(m-2)(m-3)(m-4)}{(5!)n^5}+\frac{m(m-1)(m-2)(m-3)(m-4)(m-5)}{(6!)n^6}+\ldots\pm\frac{m}{n^{m-1}}\mp\frac{1}{n^m}$$

The First two terms in the binomial expansion are identical to the exponential Taylor series. The next terms is different but for *m* sufficiently large,

$$m(m-1) \approx m^2$$

And in general for sufficiently large *m*,

$$m(m-1)(m-2)...(m-(k-1)) \approx m^k$$

The restriction on *n* is so that the term $\left(1-\frac{1}{n}\right)$ is large enough that it does not collapse to zero when it is raise to the m^{th} power.

Therefore, for $n>>m$ or sufficiently large *m* and *n*:

$$\left(1-\frac{1}{n}\right)^m \approx e^{\frac{-m}{n}}$$

Hence, the probability that a single cell in a given region will remain unobscured after *m* leaves have been uniformly distributed throughout *n* cells is:

$$\mathrm{P}\left\{\mathrm{i}^{\mathrm{th}} \text{ cell remains unobscured}\right\} = \left(1-\frac{1}{n}\right)^m \approx e^{\frac{-m}{n}}$$

4.2 Canopy Region and Binomial Distribution

Since FSO is interested in the aggregate of unobscured cells in a region, we have to define a new random variable, Y, which is the total number of cells that are unobscured. Since each cell is independent identically distributed with respect to the other cells in the region, the probability that any cell will NOT be obscured is $\exp\left(\frac{-m}{n}\right)$ and the probability that it IS obscured is $1-\exp\left(\frac{-m}{n}\right)$. The random variable Y can be modeled by the binomial distribution with the probability of a success/failure being $\exp\left(\frac{-m}{n}\right)$ and $1-\exp\left(\frac{-m}{n}\right)$ respectively.

$$\mathrm{P}\{\text{y cells unobscured}\} = \mathrm{P}\{\mathrm{Y}=\mathrm{y}\}$$

$$= \binom{m}{y}\left(e^{\frac{-m}{n}}\right)^{y}\left(1-e^{\frac{-m}{n}}\right)^{m-y}$$

The average number of unobscured cells after *m* leaves have been placed among *n* cells is the expectation of Y.

$$\mathrm{E}\{\mathrm{Y}\} = \sum_{\mathrm{y}=0}^{\mathrm{n}} \mathrm{y}\cdot\mathrm{P}\{\mathrm{Y}=\mathrm{y}\}$$

$$= \sum_{\mathrm{y}=0}^{\mathrm{n}} \mathrm{y}\binom{n}{y}\left(e^{\frac{-m}{n}}\right)^{y}\left(1-e^{\frac{-m}{n}}\right)^{m-y}$$

$$= n\left(e^{\frac{-m}{n}}\right)\sum_{y=1}^{n}\binom{n}{y-1}\left(e^{\frac{-m}{n}}\right)^{y-1}\left(1-e^{\frac{-m}{n}}\right)^{m-y-1}$$

$$= ne^{\frac{-m}{n}}$$

The expectation can be normalized to calculate the fractional unobscured cells or area in the canopy region.

$$\text{Fractional Unobscured Area} = \frac{E\{Y\}}{n}$$

$$= e^{\frac{-m}{n}}$$

The variance of Y is calculated to be:

$$Var\{Y\} = E\left\{\left(Y - E\{Y\}\right)^2\right\}$$

$$= ne^{\frac{-m}{n}}\left(1-e^{\frac{-m}{n}}\right)$$

4.3 Matlab Implementation

A numerical analysis package Matlab by Mathworks was used to develop the scenario generating simulation software. The entire code is included in the appendix. The output of the software is a canopy region that is obscured by random foliar elements. The foliar elements stop light that could be used for optical communications.

A "mesh grid" is created so that each point in the grid can represent a point in the canopy. A Gaussian intensity profile can be mapped onto the mesh grid that is proportional an intensity of a incident laser beam. The user defines the variance of

the beam intensity. If the user wants a uniform intensity across the canopy then the intensity variance is set large. This option was not used for the Monte Carlo simulation. Figure 4.2 illustrates a region of canopy containing a penetrating beam with a large variance. The effect is that the beam penetrating the canopy appears uniform. In contrast, Figure 4.3 illustrates a beam with a smaller variance; the color distribution indicates the different levels of intensity passing through the foliar elements.

The leaves are represented by ellipses with major and minor axis determined by the user in accordance with the size of the leaves in the canopy. As illustrated in Figure 4.4, A is the major axis and B is the minor of the ellipse centered at (x_0, y_0) and the area within the ellipse is defined by $\left(\frac{x-x_0}{A}\right)^2 + \left(\frac{y-y_0}{B}\right)^2 \leq 1$. The major and minor axes can be given a size distribution, $N(\mu_A, \sigma_A)$ and $N(\mu_B, \sigma_B)$, to simulate the natural conditions that exist in the forest environment. The points in the mesh grid or canopy that are obscured are set to the value of "zero" while those that are unobscured retain their non-zero values, proportional to the intensity of the beam at that point. The simulation further assumes that the photons hitting the leaves are absorbed and not transmitted through the leaf. The leaves are randomly given (x_0, y_0) ordered pairs that determine the position of the leaf in the plane according to a uniform distribution.

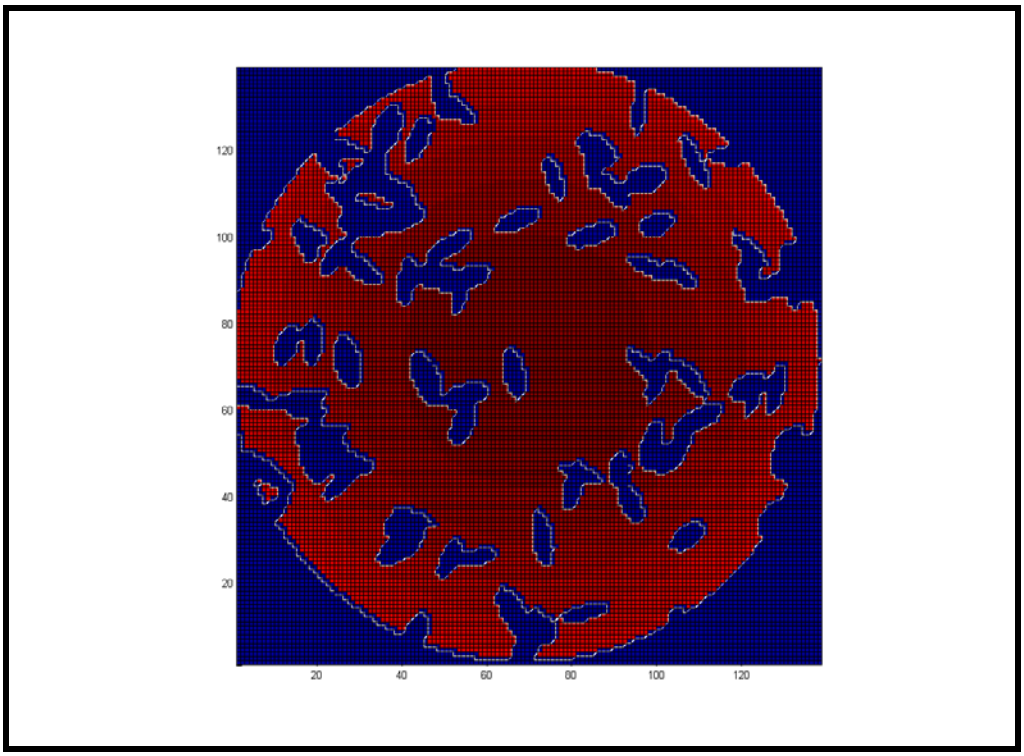

Figure 4.2 A canopy region with a uniform beam superimposed.

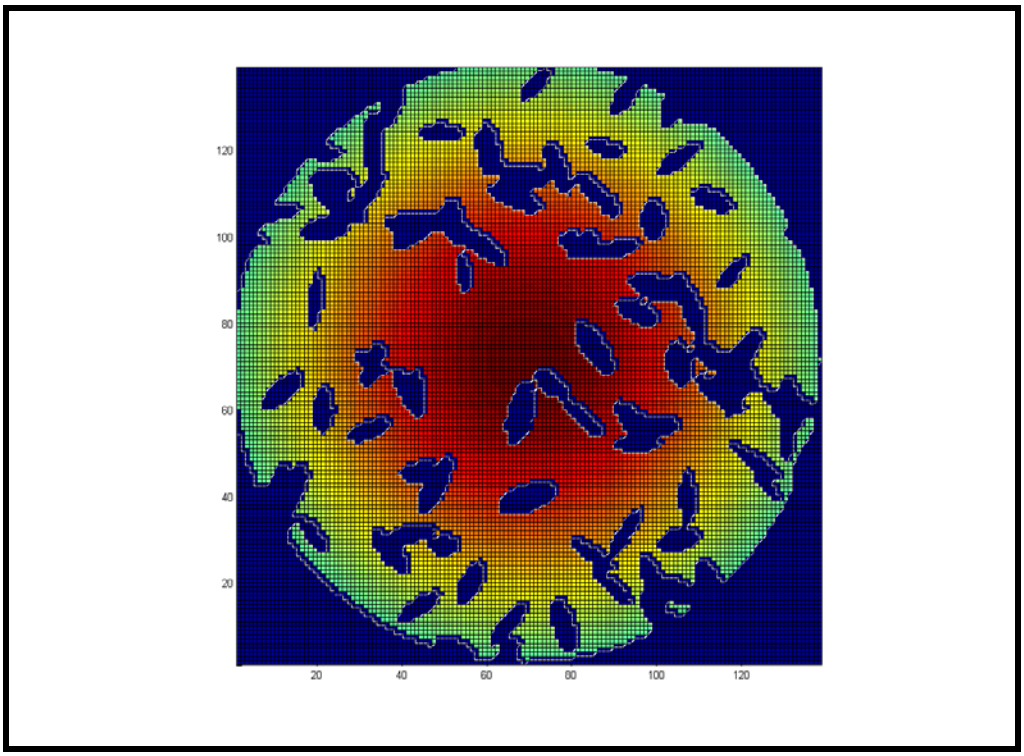

Figure 4.3 A canopy region with a Gaussian beam superimposed.

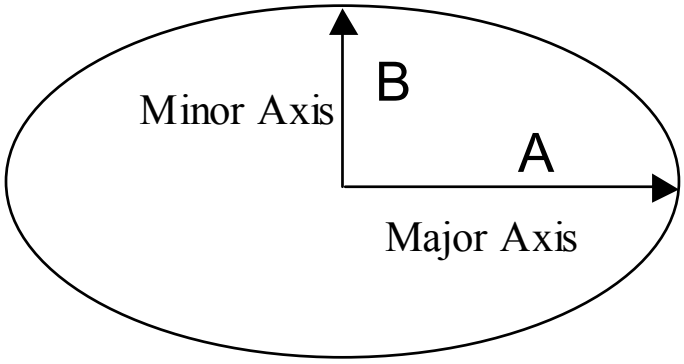

Figure 4.4 An ellipse with major axis A and minor axis B.

The ellipse's azimuthal orientation is randomly generated according to a uniform distribution between $[0, \pi]$. Also a projection angle is generated that accounts for the leaf not laying flat in the canopy and so it is projected onto the canopy according to this zenith angle. The number of leaves contained in the canopy is an input by the user but could also be randomly generated.

4.4 Monte Carlo Simulation

A Monte Carlo simulation was conducted to determine how canopy obscuration increases as the number of leaves in the canopy increases. Several different sizes of leaves were simulated including larger leaves, such as a magnolia leaf, which may have major and minor axis lengths of 12cm and 5cm respectively. Smaller leaves were also considered with more circular shapes with major and minor axes only a few

centimeters in length. The software "scenario generator" was run 1000 times for a given number of leaves in the canopy and leaf size. Each time the scenario generator ran, a statistic was recorded indicating the fractional area that was not obscured by the foliage.

After running 1000 times, a Gaussian distribution had developed. The mean and standard deviation were recorded for the specific number of leaves and leaf size in the canopy. Figure 4.5 shows the results as the foliage in the canopy becomes increasingly dense for five different leaf sizes. The unobscured area in increasingly dense foliage is clearly decreasing exponentially for the larger leaf sizes. This agrees with our analytic development of fractional area obscuration. The smallest leaf size (blue curve) appears more linear than exponential. This is because for small x

$$e^{-x} \approx 1 - x$$

The smaller leaf size results in an increased "decay-constant" that causes the fractional unobscured leaf area to decrease more slowly. Many more leaves must be added before second order effects are observed.

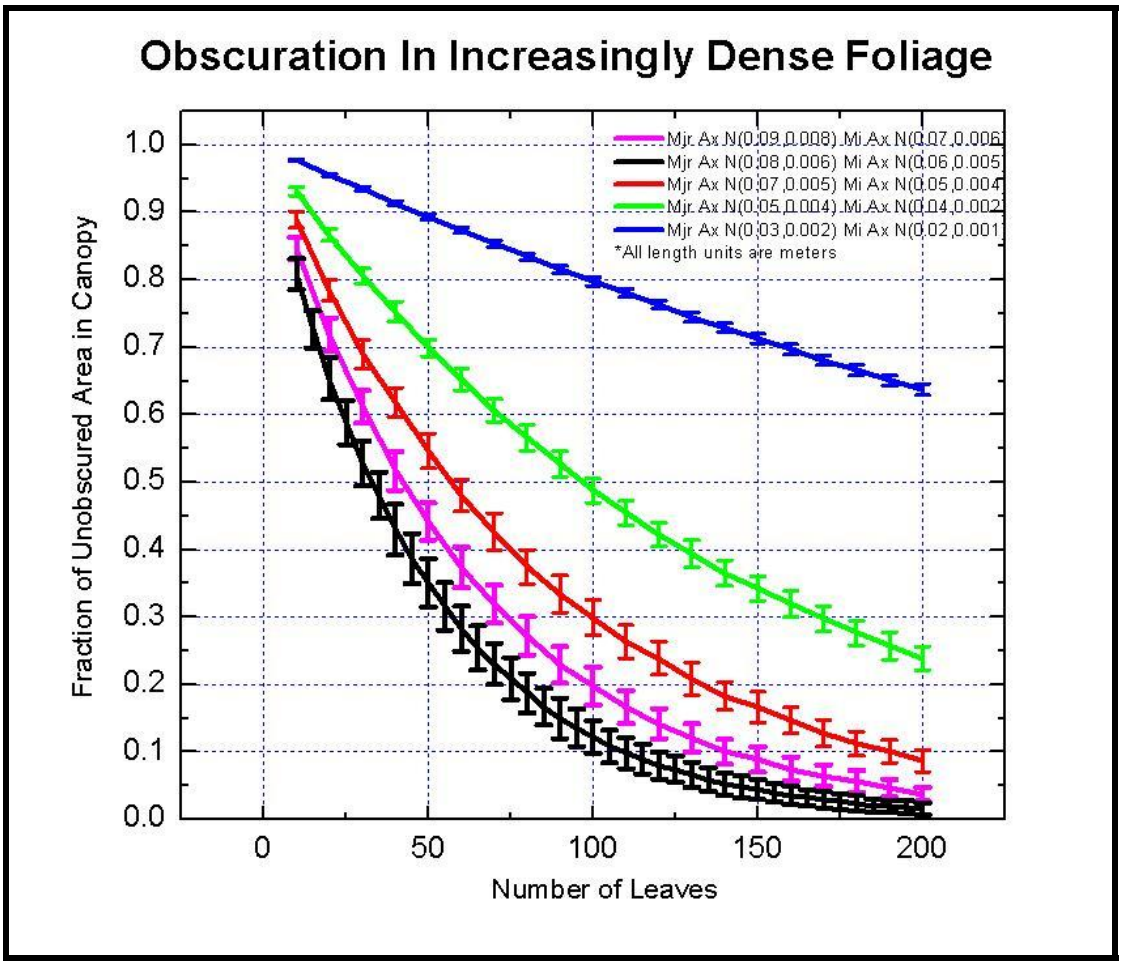

Figure 4.5 Results of Monte Carlo simulation with different leaf sizes.

Chapter 5: Passive Optical Measurements vs. Model

5.1 Leaf Transmittance

Motivated by a desire for further testing of our model and understanding actual composition of forest canopies, experimental apparatus was designed to make measurements of mature forest canopies and compare the measured data to our model. Greenbelt National Park was selected because of its proximity to the University of Maryland, College Park and because it can be classified as a "mature forest" with its canopy high above the ground.

Before proceeding with the passive optical measurements, we first wanted to test one of our assumptions regarding to leaf transmittance. The model assumes that the leaf transmittance is zero. I randomly selected 8 different types of leaf-types as seen in Figure 5.1.

Using a 4mW He-Ne laser, photodiode, photo-amplifier, and digital multi-meter, each leaf's transmittance was determined. The experimental set up and components are in Figure 5.2.

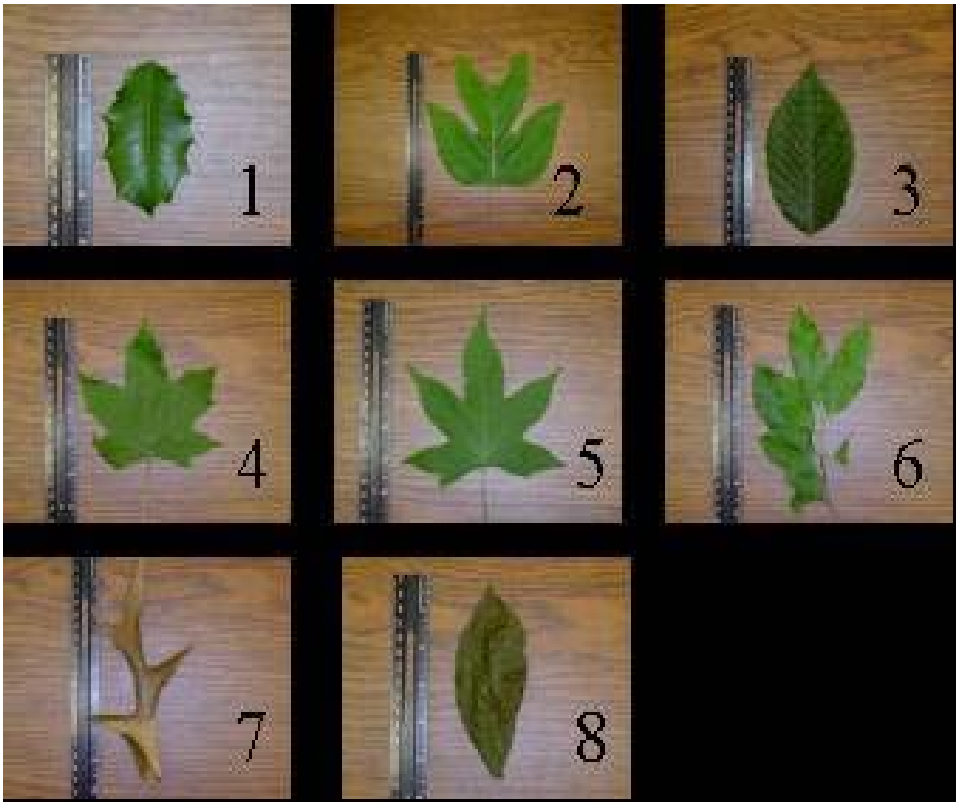

Figure 5.1 Transmittance was determined for these leaves

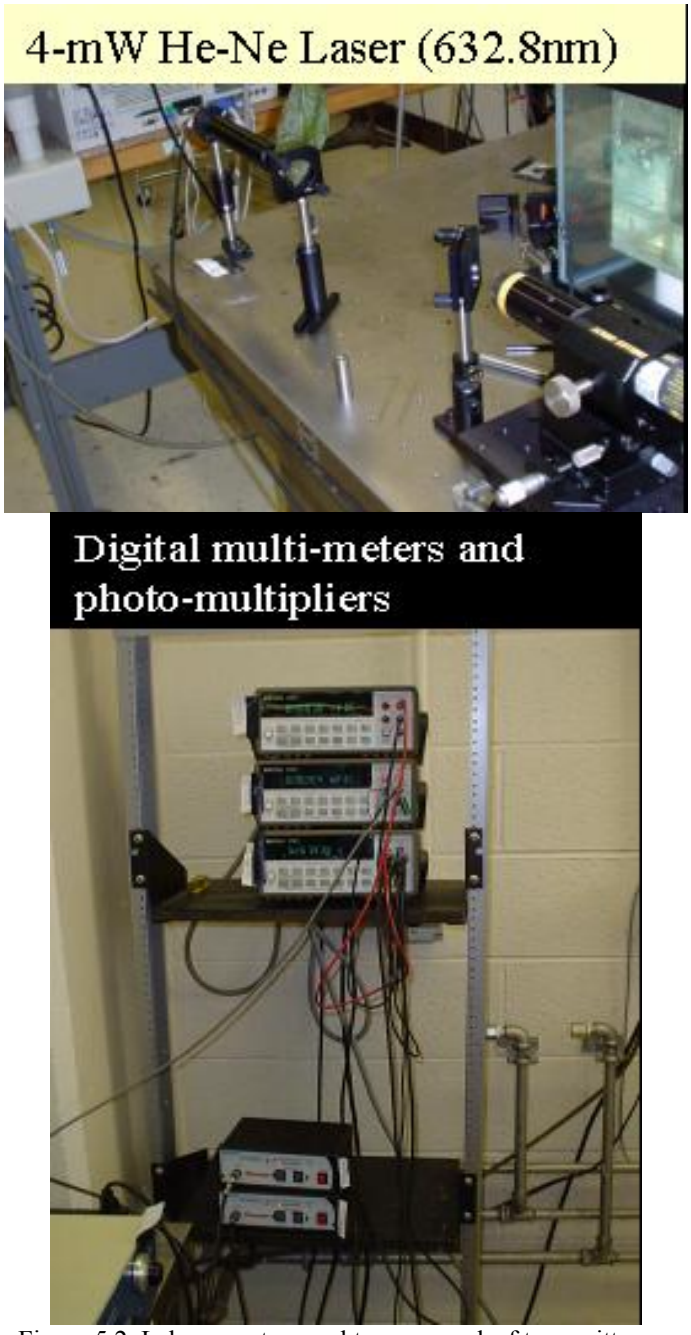

Figure 5.2 Lab apparatus used to measure leaf transmittance.

The digital multi-meter voltage was recorded while the laser was focused on the photodiode without a leaf obscuring it. The photo-multiplier was set so that it was not saturated. Each leaf was carefully laid flat in a bracket that was placed on the

floating optical table. After insuring that the leaf was correctly aligned with the system, the voltage from the multi-meter was recorded. The leaf was oriented perpendicular to the incident beam since this provided the shortest path length through the leaf and result in the greatest transmittance values. Since the voltages are proportional to the laser intensities, the transmittance is calculated by:

$$T = \frac{V_{With\ Leaf}}{V_{Without\ Leaf}}$$

Table 5.3 contains the transmittance values for the eight leaves:

Leaf	% Trans
1	0.033735
2	0.048193
3	0.042169
4	0.090361
5	0.054217
6	0.090361
7	0.060241
8	0.106024

Table 5.3 Measured leaf transmittance values

From the experimental results it is clear that the leaf is almost opaque to laser light and the model's assumption of zero transmittance is appropriate.

5.2 Passive Optical Apparatus

To measure the light penetrating through the forest canopies, an apparatus was designed to insure accurate measurement as well as portability that allowed it to be moved throughout Greenbelt Park to different sites. Figure 5.4 is a picture of the apparatus and Figure 5.5 is a schematic drawing of the apparatus, the field-of-view (FOV) of the system and the canopy above.

Figure 5.4 Passive optical measuring apparatus

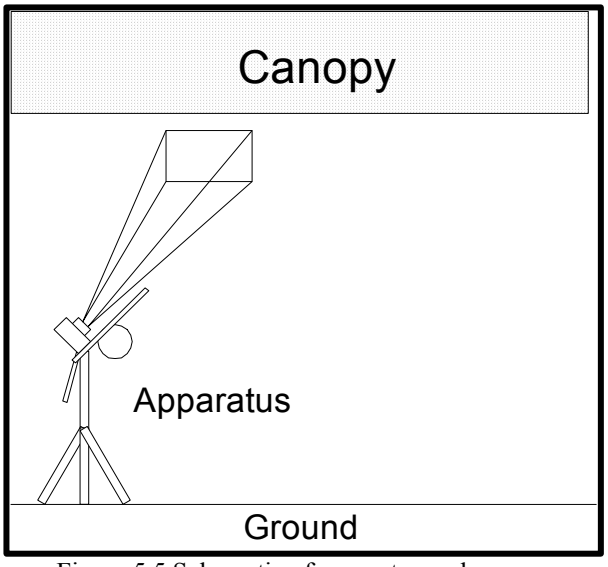

Figure 5.5 Schematic of apparatus and canopy

The apparatus has two key elements: the Sony Cyber-shot Multi-Point AF 3.2 mega-pixel digital camera and an Empire Polycast Magnetic Protractor that functions as a "plumb device." The protractor hangs toward the center of the earth and is used to determine angles without respect to level ground. The digital camera serves as a passive optical device that images the canopy onto a CCD array.

The camera is fixed to a tripod via a commercially standard screw attachment on the tripod-mounting platform and the base of the camera. A 1/8" thick steel ruler is mounted between the camera and the tripod. The system has been designed such that the ruler is perpendicular to the camera's CCD array. It is used to secure the plumb dial and to insure that the dial correctly indicates when the camera is pointed in the correct direction regardless of the grading of the ground under the tripod. Since the imaging array is looking at diffuse light penetrating the canopy, the canopy geometry, as it relates to the passive optical measurements, will be discussed in detail next.

5.3 Canopy Geometry for Passive Optical Measurements

A basic assumption of the forest canopy model is that the leaves are concentrated high above the ground and that the leaves are uniformly dense in the mature forest canopies. Our model is dependent on two parameters: m is the number of leaves in the canopy and n is the number of "cells" in the region of canopy. The parameter n is discussed in more detail in terms of its physical significance as well as a fitting

parameter. The parameter *m* can be directly related to the measurements because it is simply the number of leaves in the canopy.

Since the canopy is assumed to be uniformly dense the number of leaves being considered by the digital camera is the volume of the canopy multiplied by the canopy or foliage density.

$$\begin{aligned} \#\ \text{Leaves} &= \text{m} \\ &= \rho_{Canopy} V_{Canopy} \end{aligned}$$

V_{Canopy} is calculated by consider the difference between the two cones illustrated in Figure 5.6.

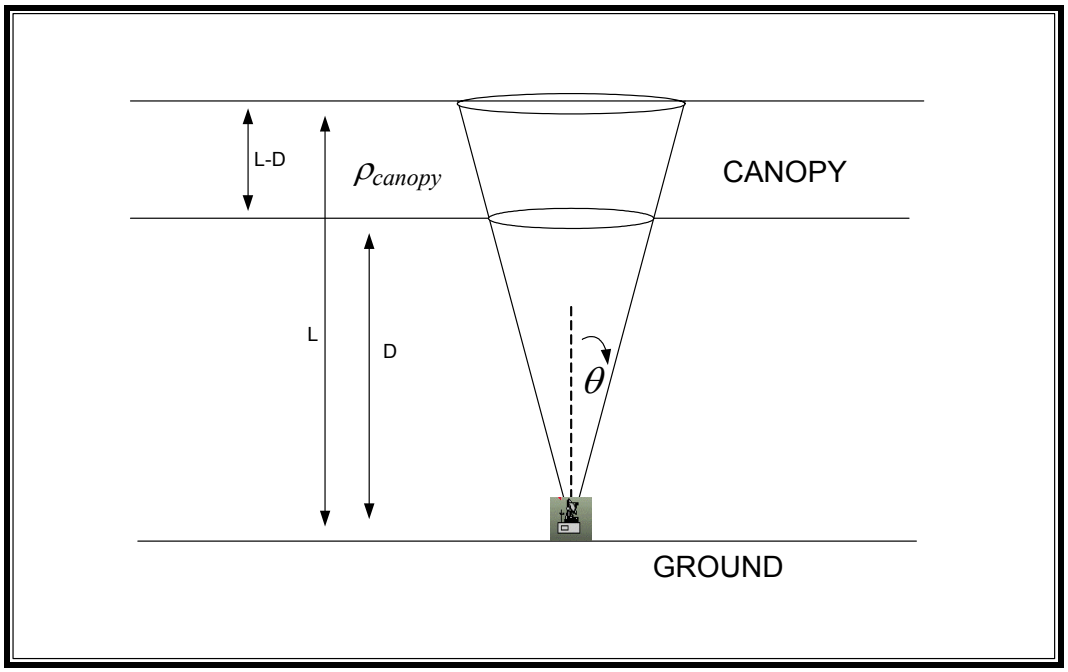

Figure 5.6 Field-of-view of camera looking straight up through the canopy.

The volume of a cone is:

$$V_{CONE} = \frac{1}{3}\pi R^2 H$$

where R is the radius of the cone and H is the height.

Considering the larger cone volume, V' the geometry requires:

$$R = L\tan(\theta)$$
$$H = L$$

Therefore,

$$V' = \frac{1}{3}\pi\left(L\tan(\theta)\right)^2 L$$
$$= \frac{1}{3}\pi L^3 \tan^2(\theta)$$

The smaller cone volume, V'', is developed in a similar manner:

$$R = D\tan(\theta)$$
$$H = D$$
$$V'' = \frac{1}{3}\pi\left(D\tan(\theta)\right)^2 D$$
$$= \frac{1}{3}\pi D^3 \tan^2(\theta)$$

The volume of the canopy is the difference between the two cones.

$$V_{Canopy} = V' - V''$$
$$= \frac{1}{3}\pi\left(L^3 - D^3\right)\tan(\theta)$$

Since the camera is looking directly vertical, the zenith angle, φ, is zero.

$$\mathrm{V}(\varphi{=}0) = \frac{1}{3}\pi\left(L^3 - D^3\right)\tan(\theta)$$

Figure 5.7 illustrates a "tilted by φ scenario" of the camera.

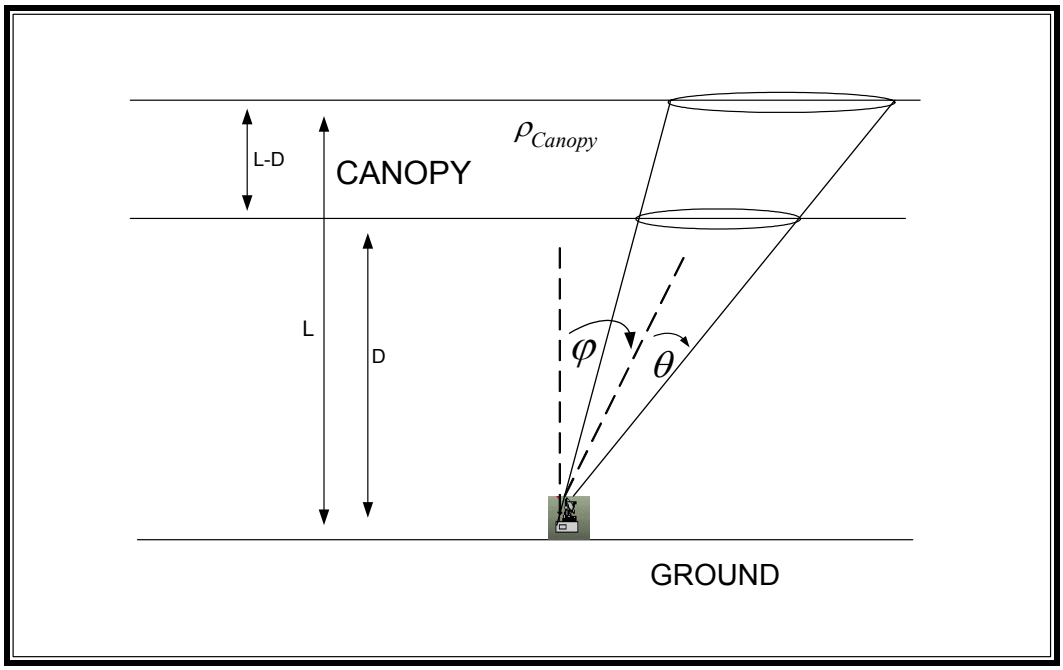

Figure 5.7 Field-of-view of camera while looking through canopy at tilted angle.

The new geometry requires some special consideration to generate the "cones" in the previous scenario. Because the canopy is uniformly dense we remove sections of the canopy in the FOV and relocate them as long as the total volume remains the same. Figure 5.8 illustrates the recreated cones in the tilted scenario.

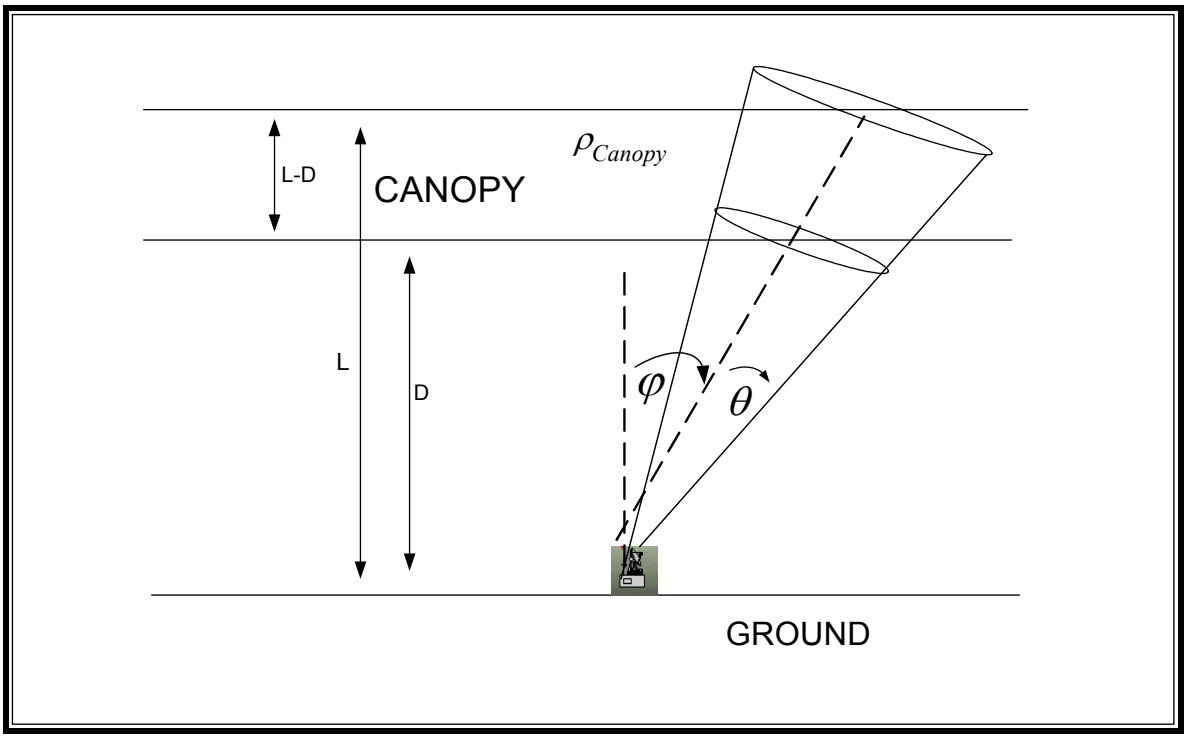

Figure 5.8 Tilted camera with symmetry argument to recreate cones

The canopy volume now has the same relationship as before only the cones have different heights, L' and D′ , and radii that are related the angle of tilt, φ , L and D.

$$V_{tilt} = \frac{1}{3}\pi\left(\left(L'\right)^3 - \left(D'\right)^3\right)\tan^2\left(\theta\right)$$

where

$$L' = \frac{L}{\cos\left(\varphi\right)} \text{ and } D' = \frac{D}{\cos\left(\varphi\right)}$$

For each canopy scenario L and D are fixed and V_{tilt} is only a function of φ

$$V_{tilt} = V\left(\varphi\right)$$

$$V(\varphi) = \frac{1}{3}\pi\left(\left(\frac{L}{\cos(\varphi)}\right)^3 - \left(\frac{D}{\cos(\varphi)}\right)^3\right)\tan^2(\theta)$$
$$= \frac{1}{3}\pi\left(L^3 - D^3\right)\tan^2(\theta)\left(\frac{1}{\cos^3(\varphi)}\right)$$

and

$$V(\varphi) = \frac{V(0)}{\cos^3(\varphi)}$$

Again the primary interest in the volume at different angles is because it can be related to the number of leaves in the camera's FOV by the canopy density. From this volumetric development and the canopy model, the fractional unobscured area (FA) can be described by:

$$FA = \%Area$$
$$= \exp\left(\frac{-m}{n}\right)$$
$$= \exp\left(\frac{-\rho V(\varphi)}{n}\right)$$
$$= \exp\left(\frac{-\rho V(0)}{n \cdot \cos^3(\varphi)}\right)$$

Thus by varying the camera's FOV zenith angle φ and sensing the fractional unobscured area, the model can be verified.

5.4 Greenbelt National Park, Greenbelt, Maryland

The location of Greenbelt Nation Park (Latitude: 39.004N, Longitude: -76.875W) was chosen because of its mature broad leaf trees and its proximity to the University of Maryland, College Park. The park has a number of footpaths that wind through the forest. The trees primarily consist of broadleaf trees such as maple, oak and sweet gum. Measurements were taken at seven different sites randomly chosen along the 1.8 kilometer long Azalea Trail. Figure 5.9 is a map of Greenbelt Park as well as the Azalea Trail.

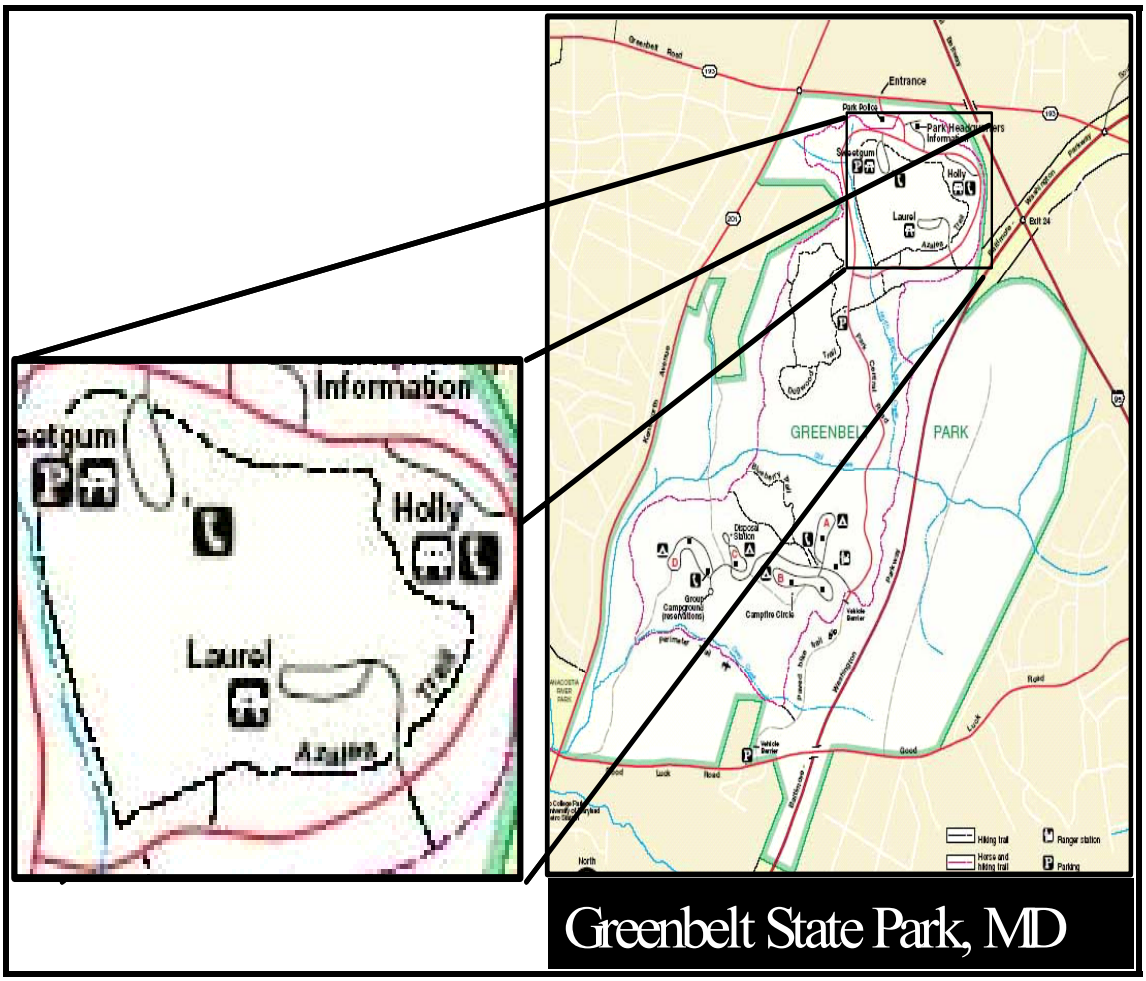

Figure 5.9 Map of Greenbelt Park and Azalea Trail.

5.5 Filtering, Image Processing, Model-Fitting

Ideal pictures show high contrast between the leaves and the sky above. The best times for measurements were close to sundown because of limited direct sunlight on the canopy. Intense diffuse light introduces shades of gray where there otherwise would be black leaves and white sky. Figures 5.10 shows pictures of high intensity diffuse light and lower intensity light as well as the corresponding grayscale histograms of the pixels in the pictures. The high intensity direct diffuse sunlight makes the image processing of the canopy less precise because it is more sensitive to the threshold value. For an image with high contrast between the leaves and sky, different threshold values between 110 and 170, only changes the fractional unobscured area by 1 percent.

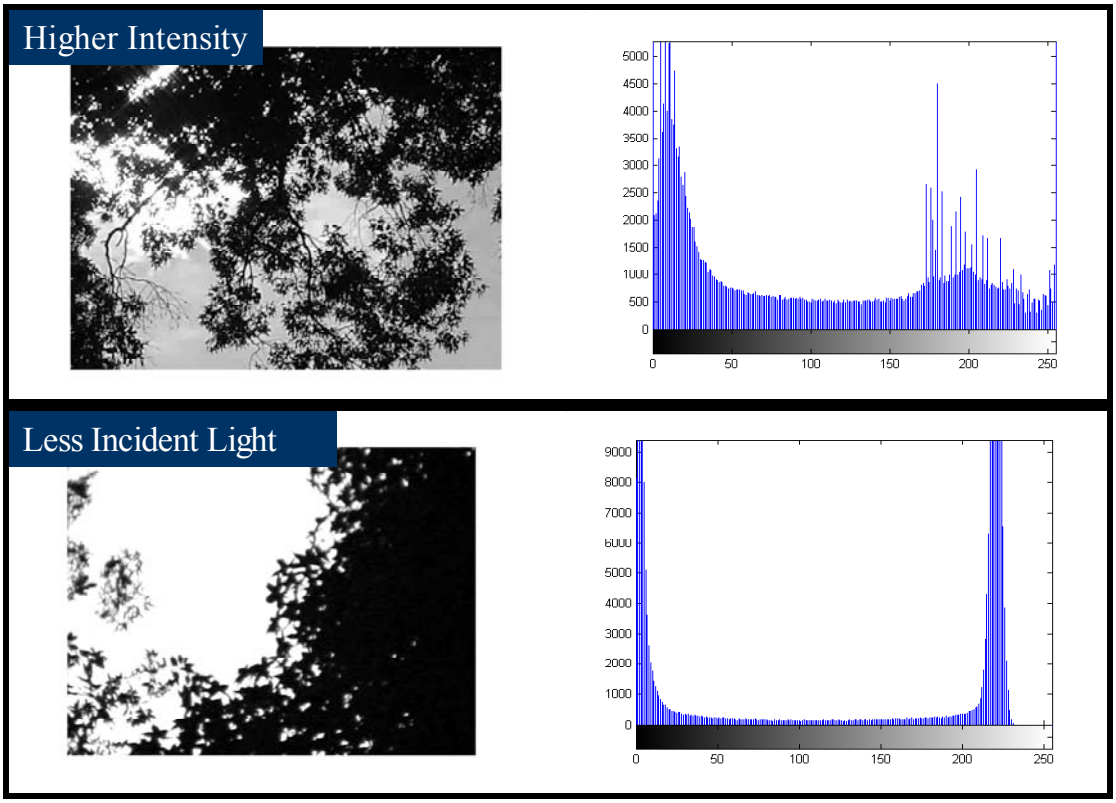

Figure 5.10 Images (taken during mid-day and at twilight) and histograms

Images were taken of the forest canopy in increments of 5 degrees with zenith angles varying from 0 to 90 degrees, starting with 0 degrees looking vertical. For each site, 19 images were taken of the canopy. As the zenith angle increases, the number of leaves in the camera's FOV increases. The images are then imported to Matlab were they are processed using a script file that passes the images through a blue filter then translates the colors to grayscale. The pixels are then sorted and tabulated according to the shades of gray.

Blue filtering was chosen for its ability to increase the contrast between the blue/white sky and the green foliar elements. The blue filtering is easily done with JPG files, which are stored in Red-Green-Blue (RGB) format. In RGB format each pixel is represented by three numbers each indicating the contribution of Red, Green, and Blue to the over all color of that pixel. By handling only the "blue" set of numbers, the image is effectively passed through a blue filter.

Grayscale (8-bit) values range between zero and 255. Once the pixels are sorted, the user sets a threshold, usually 130-160. The pixels above a threshold are counted as clear sky and those pixels below are counted as parts of obscuring leaves. Now a percentage of obscuration can be calculated for the image. This is done for each of the 19 images at each site. High contrast images, taken with low incident light, are fairly insensitive to the threshold. Once the images have been processed and the

obscuration calculated, the data can be fit to the model by adjusting the *n* value in the model.

The model development was left in the form of:

$$FA = \text{Fractional Area}$$
$$= \exp\left(\frac{-m}{n}\right)$$
$$= \exp\left(\frac{-\rho V(0)}{n * \cos^3(\gamma)}\right)$$

For fitting purposes it is helpful to define a new variable N':

$$\mathrm{N}' = \frac{\mathrm{n}}{\rho V(0)}$$

And

$$\mathrm{FA} = \exp\left(\frac{-1}{N' * \cos^3(\gamma)}\right)$$

The real fitting parameter is N' which is related to *n* by the volume and density of the canopy. As will be shown, N' is also related to the LAI. The data fitting was done with Matlab by determining which N' value minimizes the least squares error between the model and the measured data. The Matlab code is included in the appendix.

The measurements from the seven different sites along the Azalea Trail Greenbelt Park are presented in Figure 5.11 (a)-(m). The measurements are fitted to the model by determining the best parameter value for N'. An N' *vs. Error* curve is calculated for each site. Site measurements are plotted with the zenith angle on the horizontal axis and the percent-unobscured area, on the vertical axis. Overall, the measurements along the Azalea Trail were successful in showing a high degree of correlation between the percent-unobscured area and the model's predictions.

5.6 Measurements vs. Model

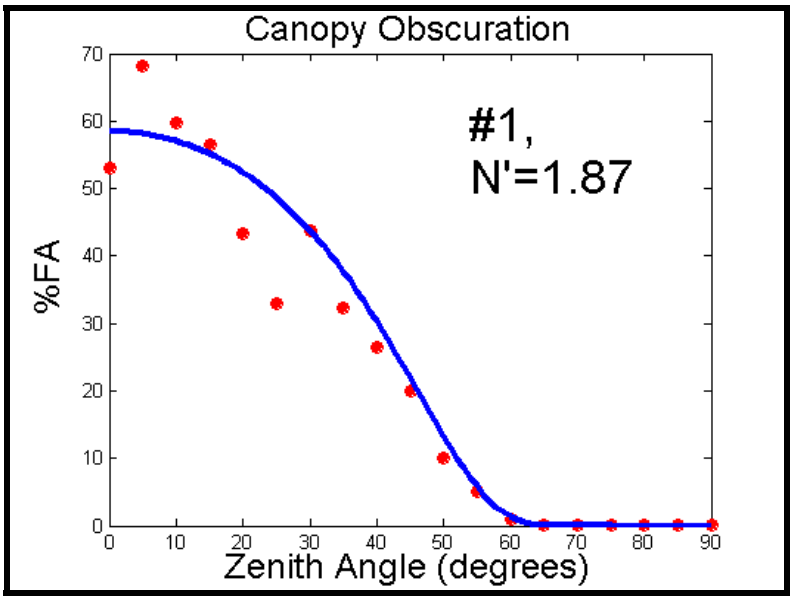

(a) Site 1: Measurements vs. Model

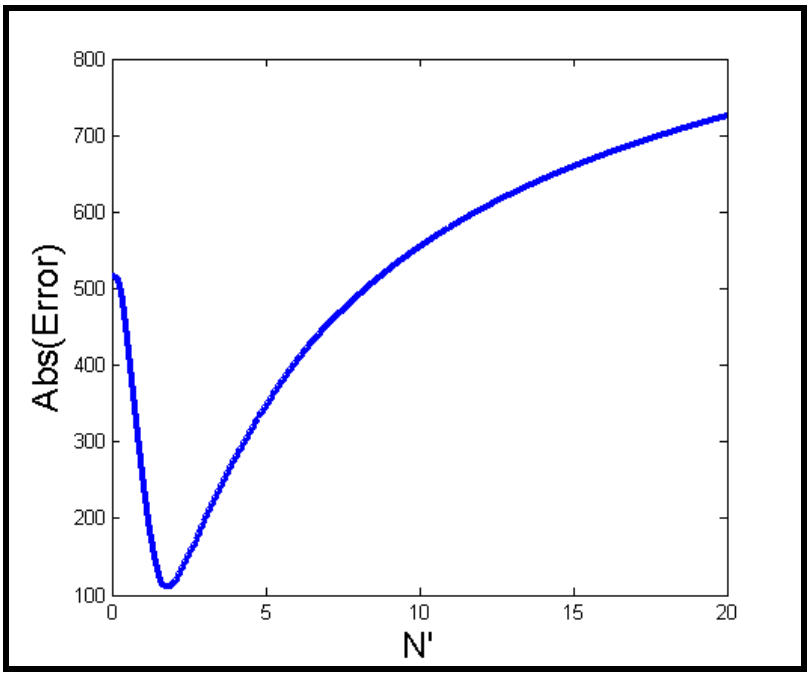

(b) Site 1: N' vs. Error

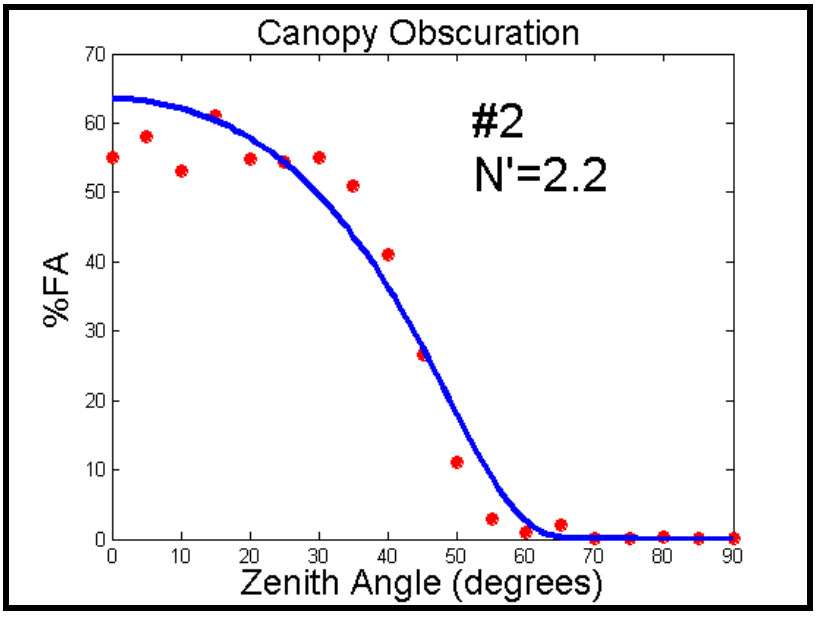

(c) Site 2: Measurements vs. Model

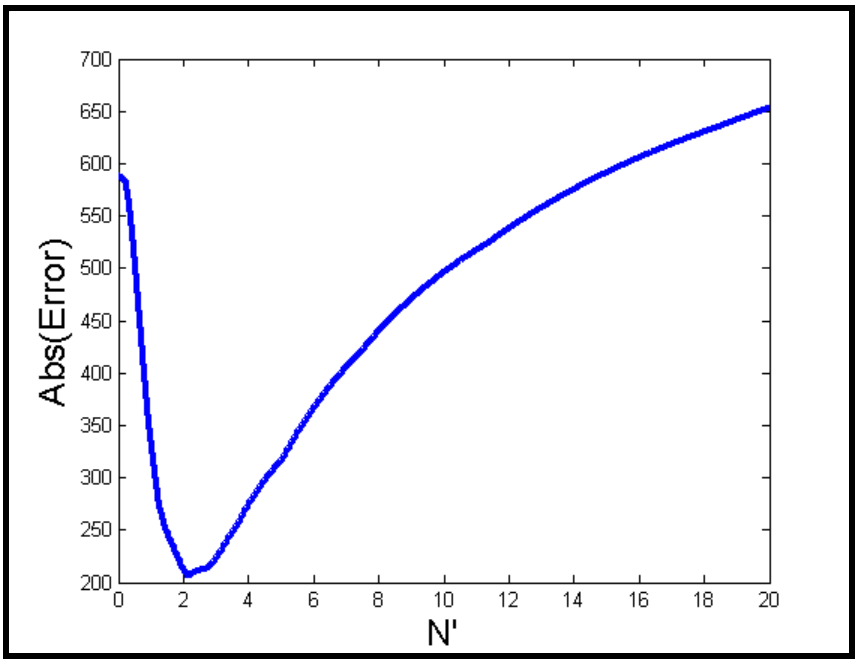

(d) Site 2: N' vs. Error

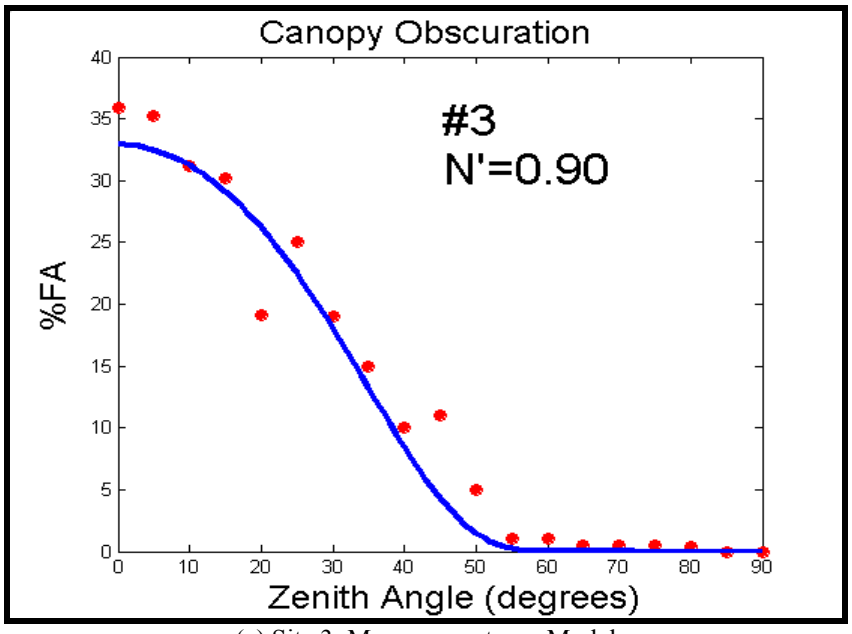

(e) Site 3: Measurements vs. Model

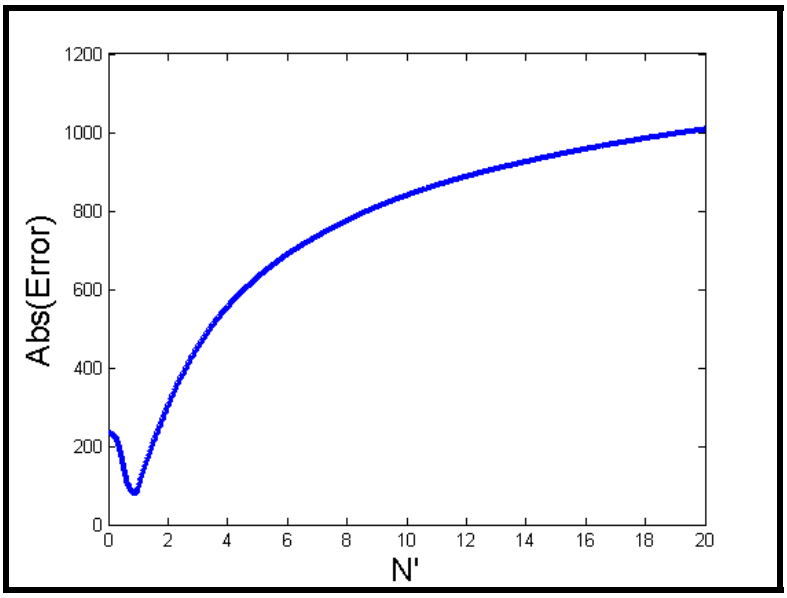

(f) Site 3: N' vs. Error

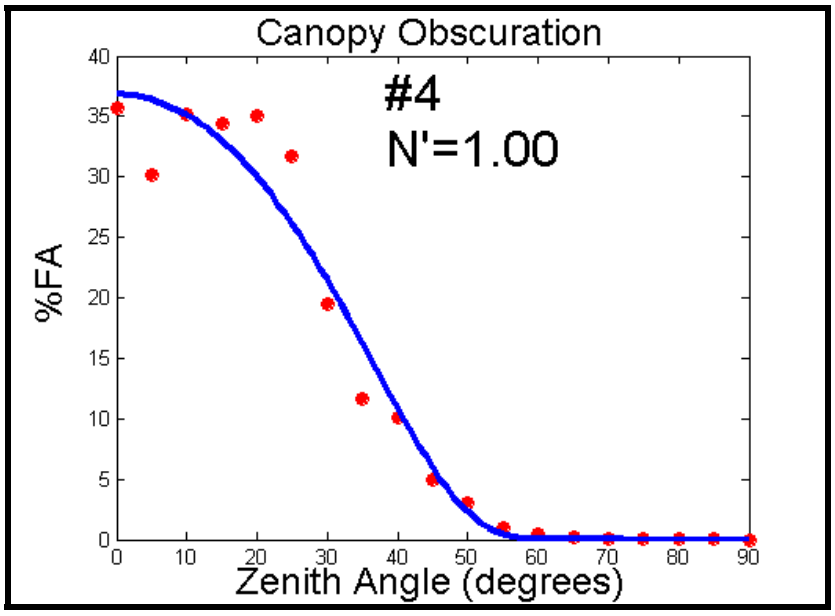

(g) Site 4: Measurements vs. Model

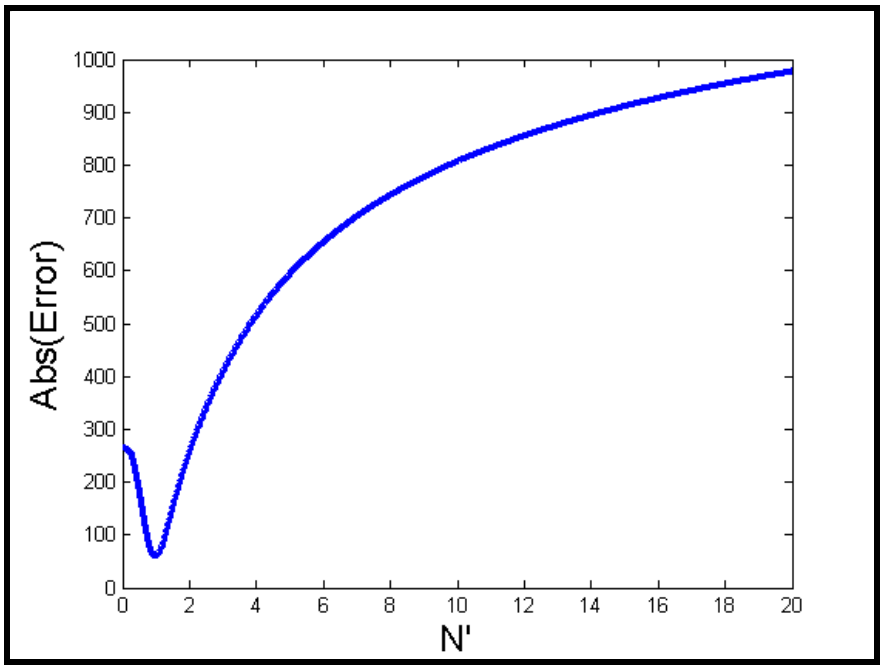

(h) Site 4: N' vs. Error

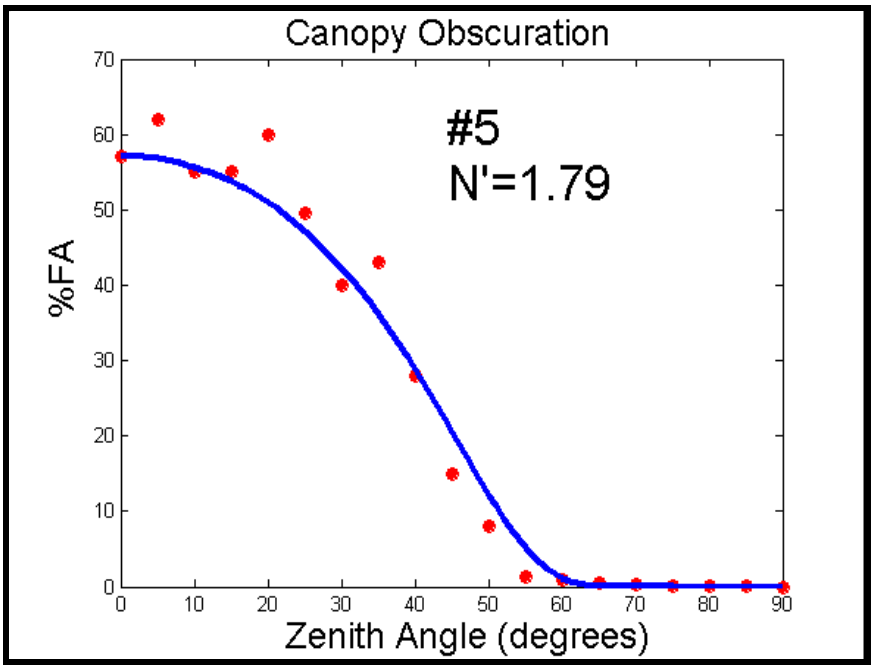

(i) Site 5: Measurements vs. Model

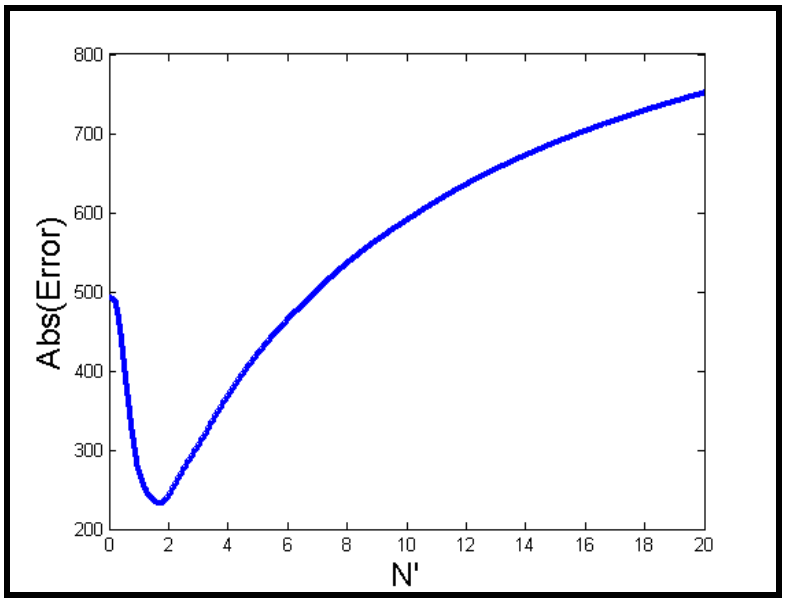

(j) Site 5: N' vs. Error

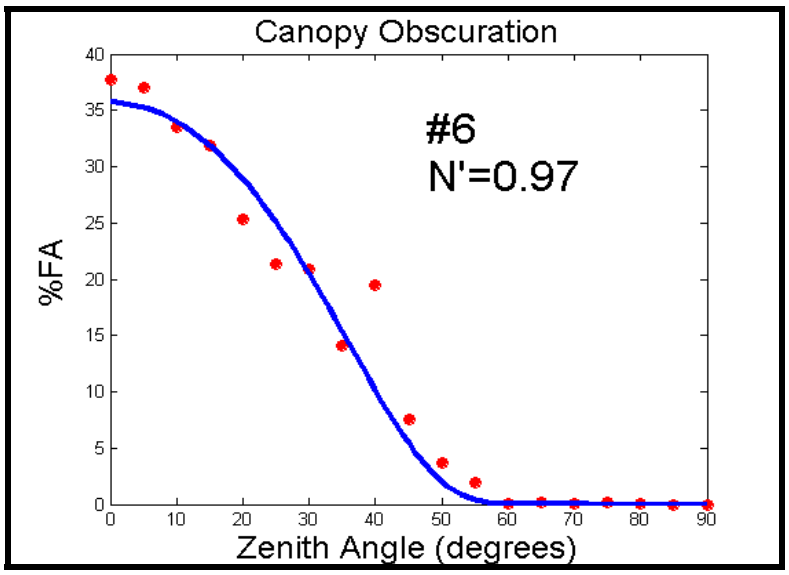

(k) Site 6: Measurements vs. Model

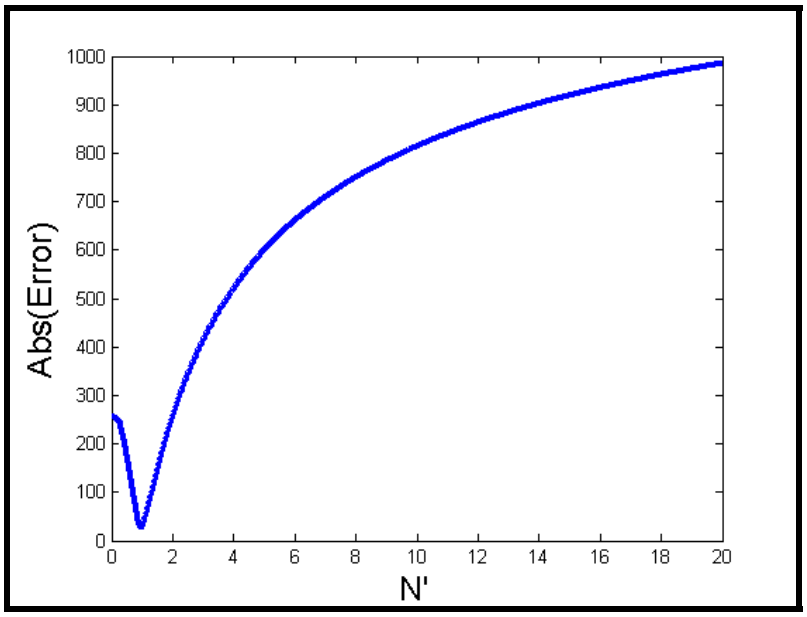

(l) Site 6: N' vs. Error

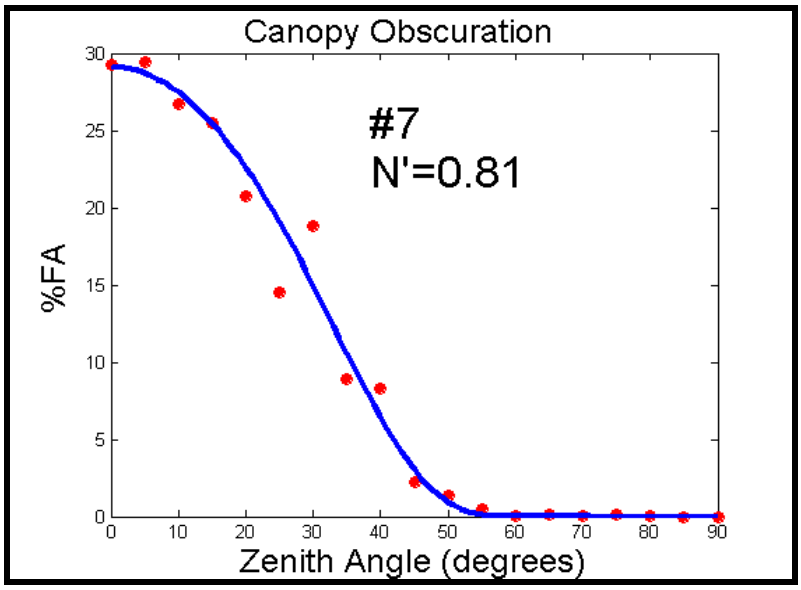

(m) Site 7: Measurements vs. Model

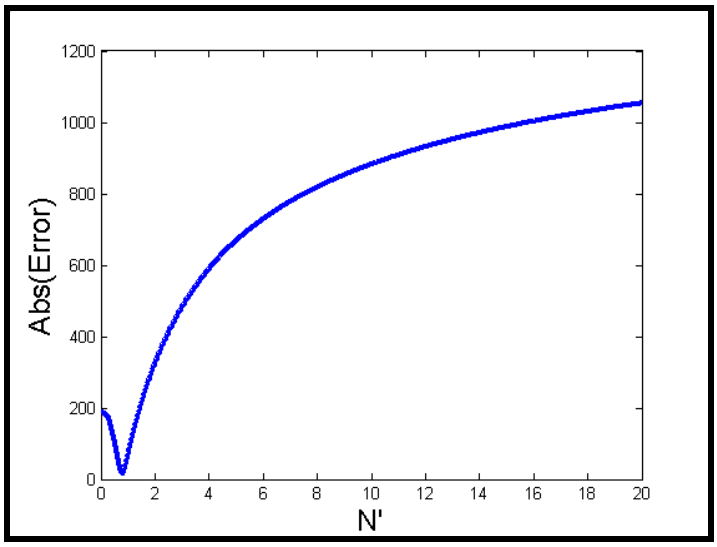

(n) Site 7: N' vs. Error

Figure 5.11 (a)-(n) Measurements vs. Fitted Model and Minimizing Error Curve for Each Site in Greenbelt National Park

The "running path" site was chosen after I observed that it appeared to have conditions that are extremely close to the assumptions of the canopy model. The foliage is concentrated high above the ground and the leaves appear to be equally distributed.

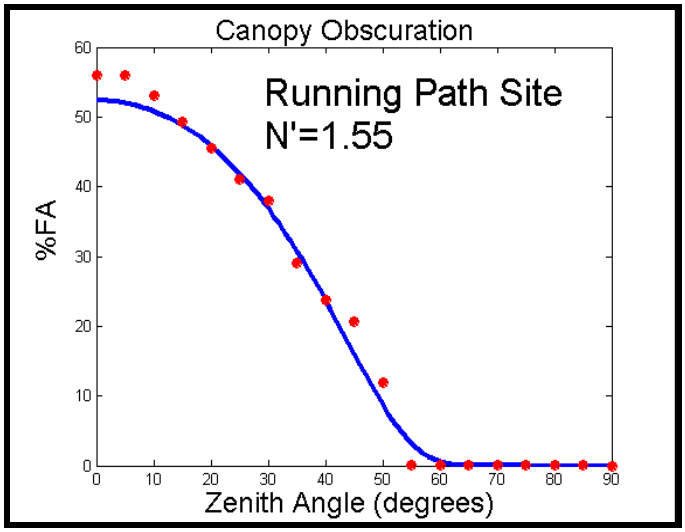

(a) "Running Path" Measurements vs. Model

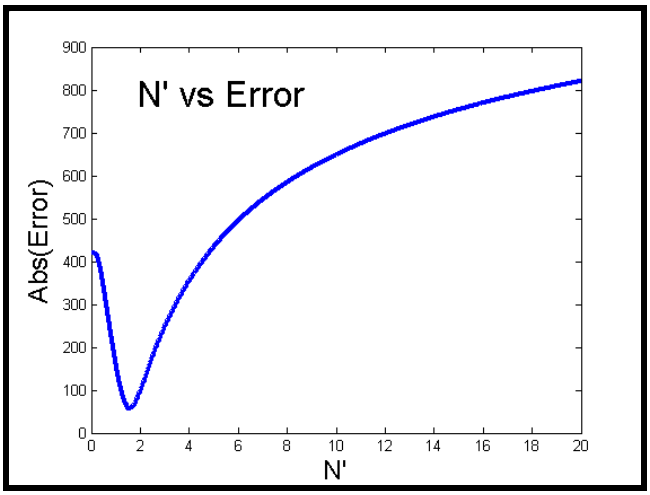

(b) "Running Path" N' vs. Error

Figure 5.12 (a)-(b) Running Path Site: Measurements and Error Curve

5.7 Site Measurement Analysis

Site 1:

Measurements were taken next to a set of parallel bars about 100 meters from the beginning of the trail. The first data point appears a lower than the following three data points as there must be a collection of leaves that exit the camera's FOV as its zenith angle increases. From zenith angles between 30 degrees and 90, there is a very close agreement between the model and measurements. It should be noted that all the site measurements from zenith angles 60 to 90 degrees is very close to zero. The N' vs. Error figure illustrates the "well-behaved" error curve that is minimized for $N' = 1.87$ value.

Site 2:

Measurements were taken next to an exercise station that was entitled "body raise station" and a large tree stump that stands about 1.3 meters high and 0.6 meters wide. Site 2 is located another 80-100 meters past Site1. Site 2 measurements follow the general curve of the model but not as closely fitted as some of the other site measurements. The error curve shows a best-fit $N' = 2.3$ value and is not as smooth as the site 1 curve.

Site 3:

Measurements were taken next to an exercise station titled "over-head latter station" and near the trail fork with one path returning to the "Sweet Gum Picnic Area." Site 3 is located another 120 meters past Site 2. Site 3 measurements have a similar quality as sites 1 and 2. The error-curve is smooth and shows a best-fit parameter $N' = 0.90$ value.

Site 4:

Site 4 is located at the Azalea Trail mile marker that reads "0.2 miles." Site 4 is located another 130-150 meters past Site 3. Site 4 measurements have a similar quality as sites 1, 2 and 3. The error-curve is smooth and shows a best-fit parameter $N' = 1.00$ value.

Site 5:

Site 5 is located on the Azalea Trail at a large manhole cover that is in the trail about 500 meters from the start of the trail. Site 5 measurements have a better quality than the previous sites and seem to be more consistent with the model curve. The error-curve is smooth and shows a best-fit parameter $N' = 1.79$ value.

Site 6:

Site 6 is located 250 meters before the end of the Azalea Trail at a sign that points to the "Holly Picnic Area." Site 6 measurements have the least cumulative error value at the best-fit N' parameter than the pervious five sites. The measurements are consistent with the model. The error-curve is smooth and shows a best-fit parameter $N' = 0.97$ value.

Site 7:

Site 7 is about 100 meters before the end of the Azalea Trail. Site 7 measurements are the best of all previous sites including Site 6. This could be in part due to the very level terrain. The measurements are consistent with the model. The error-curve is smooth and shows a best-fit parameter $N' = 0.81$ value.

Running Path Site:

The "running path" site traverses behind the University of Maryland, College Park near Baltimore Ave (Route 1) and has a long uniform canopy that envelops the path

for about 200 meters. The exact location of this site is near the Paint Branch Golf Driving Range on University Blvd (Route 193) between Metzerott Rd. and Baltimore Ave. For the seven Azalea Trail Sites the camera was never parallel with the trail so as to not have the canopy affected by the path. For the running path site, the camera's sweep followed the asphalt path. The "measurements vs. model" curve is in very close agreement but has a cumulative error that is still relatively close to Sites 6 and 7 along the Azalea Trail. The error-curve is smooth and shows a best-fit parameter $N' = 1.55$ value

5.8 Fitting Parameter N'

The fitting parameter, N', was originally defined to consolidate many constants into a single constant, but also can be directly related to LAI. We have already developed LAI to the point were it was defined as the one-sided sum of projected leaf area in a region divided by total area in that region or

$$LAI = \frac{\sum_{i=1}^{m} \left(\text{projected area of leaf } X_i\right)}{\text{Total Area in Region}}.$$

LAI was used in the context of describing uniform incident light attenuation by

$$\mathrm{I}=\mathrm{I}_0 \exp\left(-\mathrm{k} \cdot \mathrm{LAI}\right)$$

or in fractional form

$$\frac{I}{I_0} = \exp\left(-k \cdot LAI\right).$$

The probabilistic model concluded that the fractional unobscured area (FA) decreases by

$$FA = \exp\left(\frac{-m}{n}\right)$$

where *m* was the number of leaves in the region and *n* was the total area in the region divided by the average leaf size. Both of these equations arguments can be related if we define a new constant, A, as the average leaf obscuration in the region and using the mean value theorem of integration (or summation), LAI can be defined as

$$LAI = \frac{m * A}{\text{Total Area in Region}}$$

Equating the exponential arguments yields,

$$\frac{m * A}{\text{Total Area in Region}} = \frac{m}{n}$$

$$LAI = \frac{m}{n}$$

The model parameter *n* was originally defined in terms of a cells size that was the region divided by the average leaf size. We see that *n* remains consistent with that definition. T fitting parameter was N' defined by

$$N' = \frac{n}{\rho V(0)}$$
$$= \frac{n}{m}$$

Therefore, LAI can be related to our fitting parameter by

$$LAI = \frac{1}{N'}$$

Figure 5.13 shows the LAI values for the passive optical measurements.

Site	N'	Leaf Area Index (LAI)
1	1.87	0.53
2	2.3	0.43
3	0.90	1.11
4	1.00	1.00
5	1.79	0.56
6	0.97	1.03
7	0.81	1.23
Running Path	1.55	0.65

Table 5.13 N' and LAI values for measured data

The ecological literature indicates that these are viable numbers for LAI in mature North American broadleaf forests which vary between zero and 5 LAI.

Chapter 6: FSO System Implications of Model

6.1 FSO Model Implications

Chapter 2 considered a general line-of-sight FSO communication system. The link equation was developed in terms of transmitted power P_T, received power P_R, focusing factor or optical gain $F(\theta)$, range of the link R, the link loss $L(\theta)$, and the area of the receiving aperture A_R. The link equation was written as:

$$P_R = \frac{P_R \cdot F(\theta)}{4\pi R^2} \cdot L(\theta) \cdot A_R$$

In this chapter we bring the model back "full-circle" and explore the implications of the model for air-to-ground FSO links obscured by a canopy. Partial obscuration can be considered part of the Link Loss, $L(\theta)$, component of the link equation. The resulting effect is a decrease in power at the receiver. As seen in Figure 2.1, the foliage LAI, leaf size, and the receiver aperture size influence the power received.

6.2 UAV Flyover Scenario

A natural scenario for FSO communications through foliage would be a receiver on the ground trying to communicate with a UAV flying overhead. The probabilistic canopy model would allow for quantitative analysis of the canopy's effect on

received power and by extension the signal-to-noise ratio (SNR) of the communications link as the UAV transverses the sky above the receiver.

In order to simplify this simulation we assume no pointing and tracking losses and that the only Link Loss is due to the obscuring canopy. Also the UAV maintains a constant altitude and the ground is level. The simulation allows the user to define the altitude as well as the characteristics of the transmitter, receiver and canopy cover. The canopy was divided into "cells" that were defined as the average size of a leaf in the canopy.

The receiver will only receive laser light on direct line-of-sight paths to UAV. Therefore, only the area of the canopy in line-of-sight from receiver to transmitter is of interest. Because of how close the canopy is to the receiver compared to the UAV, this region of canopy is approximately the size of the receiver's aperture. Thus the aperture (or canopy region at which the receiver is pointed) can be divided into cells that are approximately the size of a leaf.

Earlier in this paper we then noted that the probability that one of these cells is obscured occurs with probability (assume k=1 for LAI expression):

$$P\left\{i^{th} \text{ cell is unobscured}\right\} = \exp\left(\frac{-m}{n}\right) = \exp\left(-LAI\right)$$

A probability expression in terms of LAI is convenient because there are existing ecological data bases that have already measured this value for different parts of the world. Once LAI is known for an area, the probability can be expressed. This probability will serve as a threshold and will determine whether a cell is obscured or unobscured. Using Matlab's uniform random generator $\left(\mathrm{U}[0,1]\right)$, a number is assigned for each cell between zero and one. If the number is less than the threshold, the cell is unobscured.

The UAV will be communicating with the receiver at different angles with respect to the ground as it passes over the canopy as seen in Figure 6.1.

As the passive optical measurements made clear, $\varphi > 0$ values result in the canopy appearing denser than if the laser-light was penetrating the canopy from $\varphi = 0$. In order to account for an increase in LAI, an "effective LAI" value is assigned when calculating the threshold for a cell at angle φ. This effective LAI is defined as

$$eLAI = \frac{LAI}{\cos\left(\varphi\right)}$$

The new threshold is

$$P\left\{i^{th} \text{ cell is unobscured}\right\} = \exp\left(-eLAI\right)$$
$$= \exp\left(\frac{LAI}{\cos\left(\varphi\right)}\right)$$

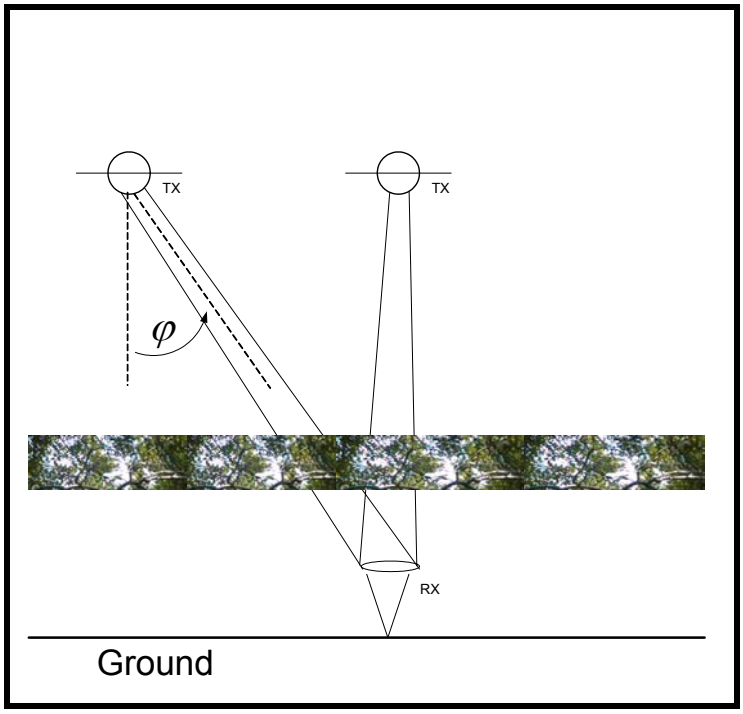

Figure 6.1 UAV flying over a receiver

With an effective LAI defined, we can now simulate a UAV sweeping overhead and cells that are available for communication according to the threshold based on the effective LAI. Once the fractional area of the aperture is determined then a signal-to-noise ratio (SNR) can be done. For this simulation the thermal noise and quantum noise are contributors to the noise term in the SNR.

The simulation described above was done for the following scenario:

UAV.Altitude = 2000 meters

UAV.Velocity = 100 meters

GEOM.Start = -5000 meters

GEOM.Stop = 5000 meters

GEOM.Delta = 100 meters

XMIT.Power = 2 Watts

XMIT.Beamwidth = 60 Degrees

XMIT.WaveLength = 1.5um

XMIT.Bandwidth = 1GHz

CANOPY.Height = 20meters

CANOPY.LeafArea = $16cm^2$

CANOPY.LAI = 0.8 Unitless

RCVR.Diameter = 10cm

DISPLAY.Ymin = -10dB

DISPLAY.Ymax = 30dB

6.3 Flyover Simulation Results

Figure 6.2 illustrates the SNR ratio in decibels as a function of the time as the aerial vehicle begins its approach overhead. Generally communication can only occur when the SNR is greater than 1 or 0dB. For the simulated scenario, the SNR is above 0dB when the plane is within 1000 meters of the receiver.

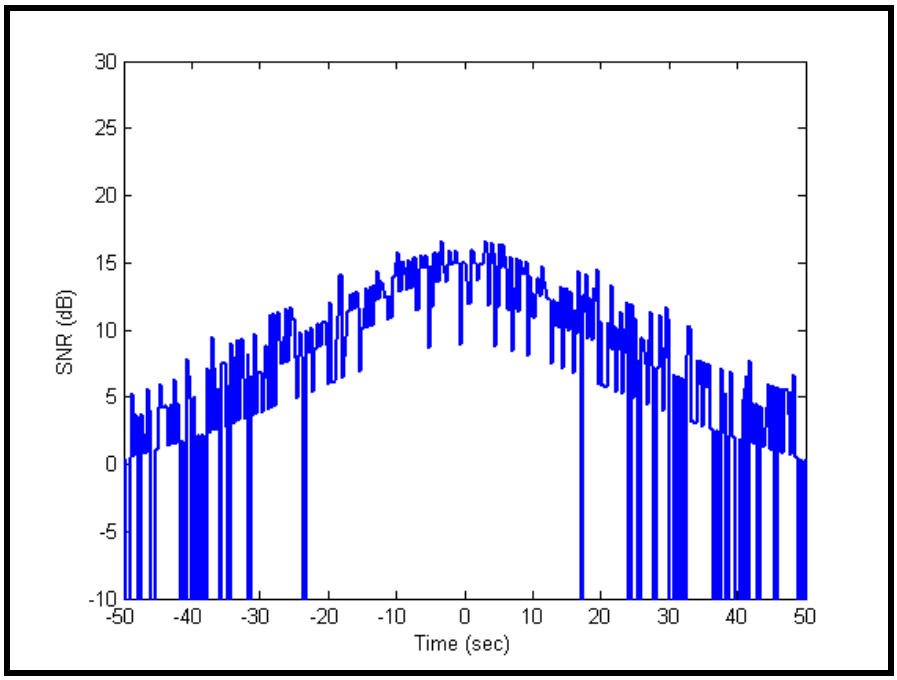

(a)

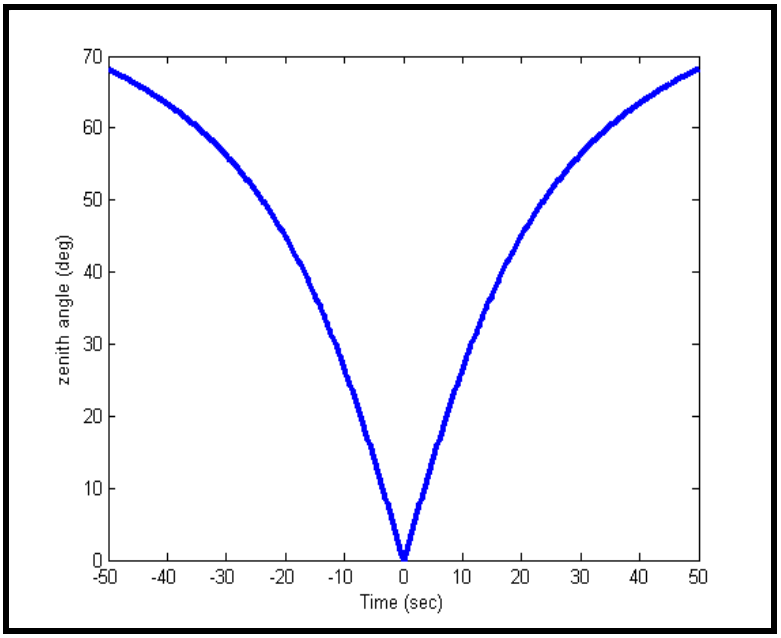

(b)

Figure 6.2 (a)-(b) SNR vs. Time and Zenith Angle vs. Time

To illustrate the sensitivity of the FSO system performance to the receiver aperture size, simulations were conducted varying the aperture from a very large aperture (50cm) to a small aperture (2cm). The velocity and height are kept constant so the "zenith angle vs. time" plot from the previous figure is the same. Figures 6.3(a)-(d) illustrate the effect of the receiver aperture size. For the large aperture diameters the unobscured area will approach the fractional unobscured area for the canopy with that effective LAI (depending on the receiver's angle looking through the canopy). As the diameter decreases the system's SNR becomes more sensitive to each cell's operational status (obscured/unobscured).

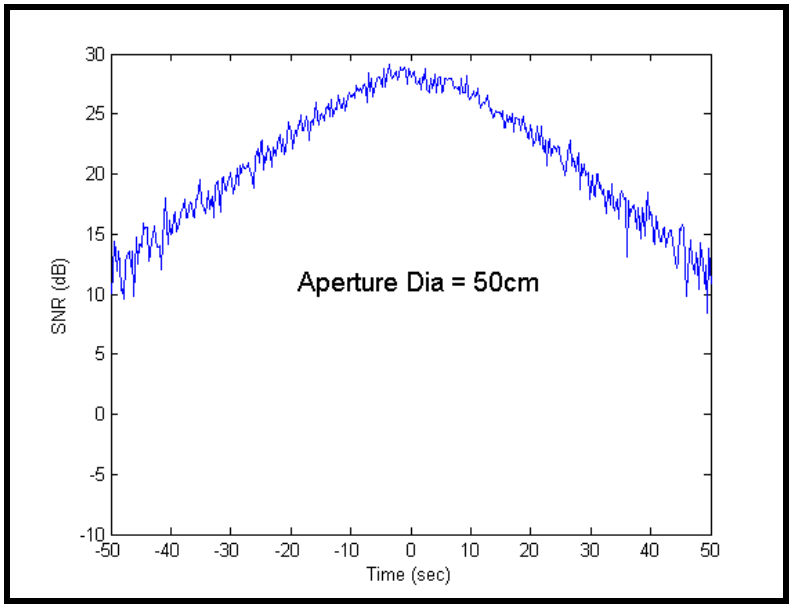

(a)

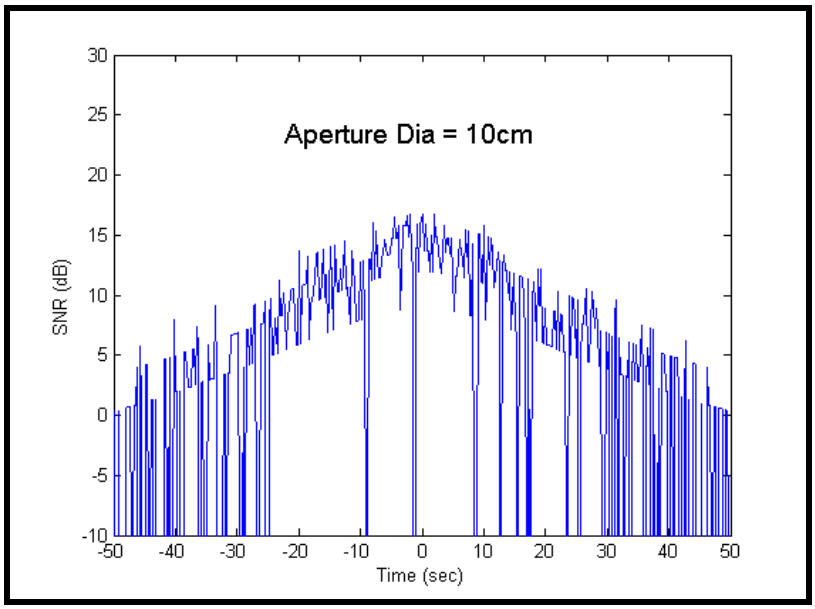
Aperture Dia = 10cm
SNR (dB)
Time (sec)
30
25
20
15
10
5
0
-5
-10
-50
-40
-30
-20
-10
0
10
20
30
40
50

(b)

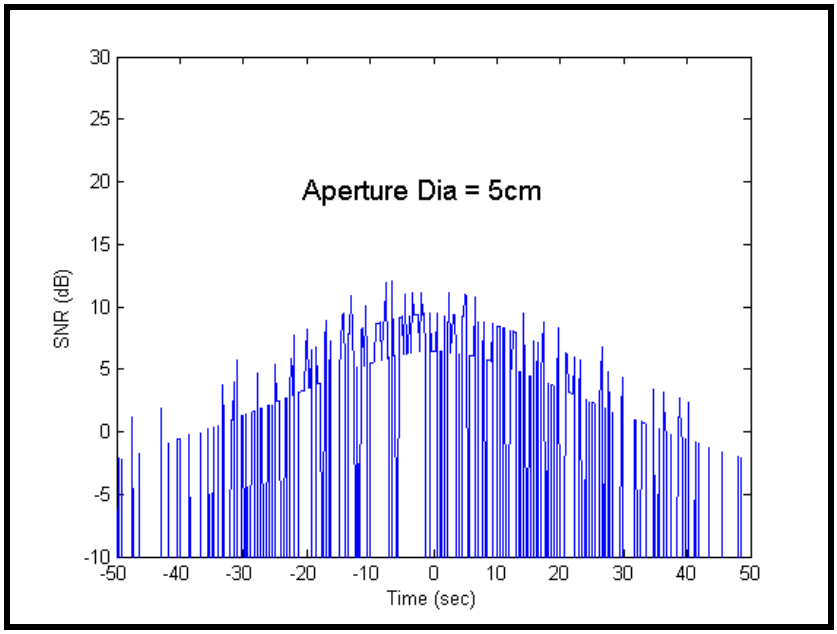
Aperture Dia = 5cm
SNR (dB)
Time (sec)
30
25
20
15
10
5
0
-5
-10
-50
-40
-30
-20
-10
0
10
20
30
40
50

(c)

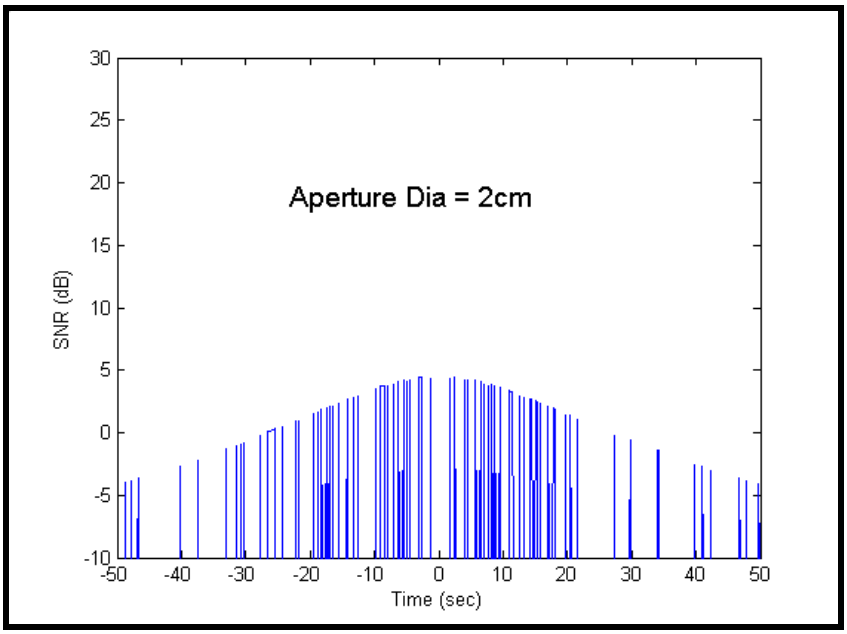

(d)

Figure 6.3 (a)-(d) Same flyover with increasingly smaller sized aperture

The limiting case is illustrated in the Figure 6.4(d), which occurs when the aperture diameter is smaller than a single leaf. The operability of the system is then described by a Bernoulli trial for each cell.

$$P\left\{i^{th} \text{ cell is unobscured}\right\} = \exp\left(-\frac{LAI}{\cos(\varphi)}\right)$$

One way to cause longer durations of operability for any system is to increase the altitude of the UAV. If the altitude is increased while the velocity of the plane remains constant, the transmitter's zenith angle will change slower. The trade-off is that the transmitted power would have to be increased to maintain the same SNR.

Chapter 7: Conclusions and Future Effort

7.1 Conclusions

Both the Monte Carlo simulations and the passive optical measurements support the probabilistic canopy model for mature broadleaf canopies. Also, it has been experimentally verified that the transmittance of broadleaf foliage can be approximated as zero. The flyover signal-to-noise ratio simulation shows promising applications for this model in communication link analysis involving mature forest canopies.

7.2 Future Efforts

There are a number of additional investigations that would be extensions of this work. Commercial-off-the-shelf (COTS) LAI measuring instruments exist and are available for purchase or rental, one example is the LAI-2000 Plant Canopy Analyzer available through LI-COR**.** This instrument could verify the LAI measurements extrapolated from the passive optical measurements. Data from the NASA VCL mission will be available from the Smithsonian Environmental Research Center (SERC) flyover site, which is close to College Park and would provide LAI measurements to compare against the passive optical measurement discussed in this paper. Also actual flyover's using manned or unmanned aerial vehicles equipped with FSO equipment

could be used to analyze and measure the canopy's effects on FSO links and may verify the SNR simulation performed in the previous chapter.

The effects of wind and wind gusts in FSO communications through foliage could be analyzed. Besides mature forests, different types of canopies could be analyzed. Also, a model could assume different leaf distributions within a canopy or foliage including a model that takes into account leaves clumping around a single branch. Vertical communications could be explored using a highly diverging beam exiting from beneath the canopy. This may apply to a search and rescue scenario with beacons and where other technologies are not sufficient. A multi-scatter model may be appropriate for a ground-to-air FSO link. This model may be based on the orientation of the leaves and more advanced stochastic and random processes.

Appendix

(Simulation Code Matlab m-files)

gaussian_spot.m is the scenario generator developed to simulate randomly placed leaves in a canopy. A laser light beam with variable intensity can be superimposed on the light beam.

```
function [number_of_pixels_unobscured, pix]=gaussian_spot(Pixels, beam_dia, P, w,
Maj_mu, Min_mu, Maj_stdev, Min_stdev, Layers, leaves)
% function feb04_gaussian_spot(Pixels, beam_dia, P, w, Maj_mu, Min_mu,
Maj_stdev, Min_stdev, Layers)
% test line: [unob_pix, pix]=feb04_gaussian_spot(5e3, 1, 1, 1.2, .1, .08, .005, .003, 1,
15)
%
%
% Pixels = one dimesion of square matrix or pixels , beam_dia = laser beams
diameter
% Maj_mu = average size of leafs' semi-major axis, Min_mu = average size of leafs'
minor axis
% Maj_stdev = semi-major axis standard deviation, Min_stdev = Minor axial
standard deviationm
% P = Maximum Power, w = spot radius, Layer = Layers to be superimposed
% gaussian_spot_norm.m
% normal distribution of size of leaves
% gaussian intensity distribution
%
% UPDATED: 28 Feb 2004
% Clint Edwards
% University of Maryland, College Park

%%%%%%%%%%%%%%%%%%%%%%%%%%%%%%%%%%%%%%%%%%%%%%%%%%
%%%%%%%%%%%%%%%%%%%%%%%%%%%%%%%%%%%%%%%%%%%%%
Io = (2*P)./(pi*w^2);

nnn = 1;  %initialize Layers counter

N = ceil(sqrt(4*Pixels/pi));        % N = dimensions of the array (NxN)
del_X = beam_dia/(N-1);             % delta x is the distance between two points
del_Y = beam_dia/(N-1);             % del_x = del_y => square pixel pattern
Xo = ((N-1)/2)*del_X;               % center of beam on the x-axis
Yo = ((N-1)/2)*del_Y;               % center of beam on the y-axis
```

```
X = ones(1,N)'*[1:N]*del_X;                    % 2D matrix that contains the x position
away from the lower left corner which is the origin
Y = flipud([1:N]')*ones(1,N)*del_Y;            % 2D matrix that contains the y position
away from the lower left corner which is the origin

I = Io*exp(-(1/2)*((X-Xo).^2+(Y-Yo).^2)/w^2);                % maximum intensity at
center of beam

Beam_Disc = (X-Xo).^2+(Y-Yo).^2 <= (beam_dia/2)^2;    % selects pixels that are
inside beam and sets them as "1" and all others "0"

pix = sum(Beam_Disc);        %total number of pixels in beam
pix = sum(pix);

B = Beam_Disc.*I;    % projection of beam intensity onto beam disc
B = sum(B);          % sum 2D array to colum vector
B = sum(B);          % sum colum to scalar that is the total intensity of beam
Total_Leaves = 0;              % initialize counter

NObscured_beam = Beam_Disc;
Itotal = Beam_Disc;

while nnn<=Layers    % execute for each layer
NObscured_beam = Beam_Disc;

Total_Leaves = Total_Leaves+leaves;                %total number of leaves for all
layers in current and previous layer

% fprintf('**********************OUTPUT
LAYER%4.0f**************************\n', nnn)
% fprintf('The total amount of intensity in unobscured beam is %8.2f\n', B)
% fprintf('The total number of leaves is: %8.0f\n', leaves)

An = (Maj_mu+(Maj_stdev*randn(1,leaves))).*cos(pi*rand(1,leaves)/4);
        while An<=.001                              % check to insure that
An>threshold, An is the random eliptical major axis of leaf
                An =
Maj_mu+(Maj_stdev*randn(1,leaves)).*cos(pi*rand(1,leaves)/4);
        end
        Bn = Min_mu+(Min_stdev*randn(1,leaves)).*cos(pi*rand(1,leaves)/4);
        while Bn<=0.001                             % check to insure that Bn>0, Bn
is the minor axis
                Bn =
Min_mu+(Min_stdev*randn(1,leaves)).*cos(pi*rand(1,leaves)/4);
        end
```

```
Xn = beam_dia*rand(1,leaves);                    % uniform distribution of leaves
accross laser beam
Yn = beam_dia*rand(1,leaves);                    % uniform distribution of leaves
accross laser beam
theta = pi*rand(1,leaves);                  % uniform distribution of "tilt" of elipse
n = 1;

while n<=leaves
        Leaf = ((X-Xn(1,n)).*cos(theta(1,n))+(Y-
Yn(1,n)).*sin(theta(1,n))).^2/An(1,n)^2+...
        (-(X-Xn(1,n)).*sin(theta(1,n))+(Y-
Yn(1,n)).*cos(theta(1,n))).^2/Bn(1,n)^2>=1 ;          %Bn An Xn Yn and theta
are all randomly generated

        HHH = Beam_Disc&Leaf;

while HHH==Beam_Disc      %selects new leaf if beam_disc remains unchanged
        An(1,n) = (Maj_stdev*randn+Maj_mu).*cos(pi*rand(1)/4);          %An
major/minor axis of leaf
                while An(1,n)<=0.001
                        An(1,n) = (Maj_stdev*randn+Maj_mu).*cos(pi*rand(1)/4);
                end
        Bn(1,n) = (Min_stdev*randn+Min_mu).*cos(pi*rand(1)/4);
        %Bn minor/major axis of leaf
                while Bn(1,n)<=0.001
                        Bn(1,n) = (Min_stdev*randn+Min_mu).*cos(pi*rand(1)/4);
                end

        Xn(1,n) = rand;
        Yn(1,n) = rand;
        theta(1,n) = pi*rand(1);
        Leaf = ((X-Xn(1,n)).*cos(theta(1,n))+(Y-
Yn(1,n)).*sin(theta(1,n))).^2/An(1,n)^2+...
        (-(X-Xn(1,n)).*sin(theta(1,n))+(Y-
Yn(1,n)).*cos(theta(1,n))).^2/Bn(1,n).^2>=1;
        HHH = Beam_Disc&Leaf;

end

Leaf  = flipud(Leaf);

NObscured_beam = NObscured_beam&Leaf;
Itotal = Itotal&Leaf;
```

```
n = n+1;
end

NObscured_beam = NObscured_beam.*I;              %displays data correctly on surf
plot
Itotal = Itotal.*I;
% figure
% surf(NObscured_beam)
% axis tight
% axis square

index = find(NObscured_beam ~= 0);
number_of_pixels_unobscured = length(index);

% fprintf('Total number of unobscured pixels are: %8.0f\n',
number_of_pixels_unobscured)
D = 100*number_of_pixels_unobscured/pix;
fprintf('Percent of Unobscured to Pixels:%6.6f\n', D)

A = sum(NObscured_beam);
A = sum(A);
% fprintf('Total Amount of Gaussian Radiance Unobscured: %8.2f\n\n', A)
C = 100*A/B;
% fprintf('Percent of Unobscured to Total Gaussian Radiance:%6.6f\n\n', C)

nnn = nnn+1;
end

figure
surf(Itotal)
axis tight
axis square

% fprintf('********************  RESULTS OF ALL%4.0f LAYERS
**********\n', Layers)    %superposition of all other layers
index = find(Itotal ~= 0);
number_of_pixels_unobscured = length(index);
% fprintf('The total amount of intensity in beam (without leaves) is %8.2f\n', B)
% fprintf('Total number of pixels are: %8.0f\n', pix)

% fprintf('Total number of unobscured pixels are: %8.0f\n',
number_of_pixels_unobscured)
A = sum(Itotal);
A = sum(A);
% fprintf('Total Amount of Gaussian Radiance: %8.2f\n', B)
```

```
% fprintf('Total Amount of Gaussian Radiance Unobscured: %8.2f\n\n', A)
C = 100*A/B;
% fprintf('Percent of Unobscured to Total Gaussian Radiance:%6.6f\n\n', C)
% fprintf('Total Number of Layers:%4.0f\n', Layers)
% fprintf('Total Number of Leaves:%4.0f\n', Total_Leaves)
```

Monte Carlo Simulation Script File

```
%FILENAME:  Monte_Car.m
%monte carlo simulation using feb04_gaussian_spot
%
%Program runs feb04_gaussian_spot several times and generates txt file with
statistics
%of number of % of total pixels obscured (and others)
%
% UPDATED: 19 May 2004
% Clint Edwards
% University of Maryland, College Park

n = 100;     %number of times feb04_gaussian_spot is executed and results in n data
points being generated.
bin = 30;    %number of bins for histogram

nleaf = [10:50:410];
mm = length(nleaf);
statTable = zeros(mm,3);

for m=1:mm
PixTable = zeros(n,3);
for i = 1:n

        [unob_pix, pix]=feb04_gaussian_spot(20e3, 1, 1, .9, .03, .015, .002, .001, 1,
nleaf(1,m));
        percPix = unob_pix/pix;
        line = [unob_pix, pix, percPix];
        PixTable(i,:) = line;
end
[N,X] = hist(PixTable(:,3),bin);

NN = sum(N);
normN = N/NN;
expect = X*normN';
```

```
Vari = ((X.^2)*normN')-expect^2;

statTable(m,:) = [nleaf(m),expect, sqrt(Vari)];
end

save Lim_May19a.txt statTable -ascii -tabs

for m=1:mm
PixTable = zeros(n,3);
for i = 1:n

        [unob_pix, pix]=feb04_gaussian_spot(20e3, 1, 1, .9, .04, .015, .002, .001, 1,
nleaf(1,m));
        percPix = unob_pix/pix;
        line = [unob_pix, pix, percPix];
        PixTable(i,:) = line;
end
[N,X] = hist(PixTable(:,3),bin);

NN = sum(N);
normN = N/NN;
expect = X*normN';
Vari = ((X.^2)*normN')-expect^2;

statTable(m,:) = [nleaf(m),expect, sqrt(Vari)];
end

save Lim_May19b.txt statTable -ascii -tabs

for m=1:mm
PixTable = zeros(n,3);
for i = 1:n

        [unob_pix, pix]=feb04_gaussian_spot(20e3, 1, 1, .9, .03, .025, .002, .001, 1,
nleaf(1,m));
        percPix = unob_pix/pix;
        line = [unob_pix, pix, percPix];
        PixTable(i,:) = line;
end
[N,X] = hist(PixTable(:,3),bin);

NN = sum(N);
normN = N/NN;
expect = X*normN';
Vari = ((X.^2)*normN')-expect^2;
```

```
statTable(m,:) = [nleaf(m),expect, sqrt(Vari)];
end

save SVE_FILENAME.txt statTable -ascii -tabs
```

Image Processing Code

ImProc.m used to handle the images taken from site measurements at Greenbelt park. Fractional unobscured area is calculated for each measurements as well as fitted to the model curve and the best-fit N′ determined.

```
function ImProc(StartStr,NumFiles);
% FILENAME: ImProc.m
% AUTHOR: Clint Edwards, University of Maryland, College Park
% DATE: 9 June 2004

%Find and extract extension
ExtStr=StartStr(findstr(StartStr,'.'):end);
%Strip away extension
StartStr(findstr(StartStr,'.'):end)='';
%Find location of non-numeric leading terms
Index=find(double(StartStr)<48|double(StartStr)>57);
%Save non numeric terms
LeadingStr=StartStr(Index);
%Eliminate non numeric terms
StartStr(Index)='';
%Get number of digits in numeric part
s=size(StartStr,2);
%Create vector as sequence of 19 number
NumVec=[str2num(StartStr):str2num(StartStr)+NumFiles-1].';
%Restore leading zeros by first adding 10^s
NumVec=NumVec+10^s;
%Convert vector from num to str
StrVec=num2str(NumVec);
%Eliminate leading 1 character
StrVec(:,1)=''
%Add extension into vector string
ExtVec=ones(size(StrVec,1),1)*double(ExtStr);
StrVec=[StrVec,char(ExtVec)];
%Add Leading String into vector string
LeadingVecNums=ones(size(StrVec,1),1)*double(LeadingStr);
StrVec=[char(LeadingVecNums),StrVec,];

I = StrVec;
celldata = cellstr(I);
SS = length(celldata);
incre = 5;  % incre is the degree difference between two succeeding images
ang = (SS-1)*incre;
Angle = [0:incre:ang]';
```

```
perc_pen = zeros(SS,2);
perc_pen(:,1) = Angle;
for j=1:SS(1)
P = imread(I(j,:));
% figure
% imshow(P(:,:,3))
% figure
% imhist(P(:,:,3))
Light = find(P(:,:,3)>140);
[A B] = size(P(:,:,3));
den = A*B;
nom = length(Light);
perc_pen(j,2) = 100*nom/den;

end

% exp_pen = sum(perc_pen)/length(perc_pen);
% std_pen = std(perc_pen);
% save “Filename.txt”  perc_pen -ascii -tabs %SAVE ...  -ASCII -TABS  delimits
with tabs.

Dat = perc_pen;
n =[0.01:.0001:20]';
len_n = length(n);
error = zeros(len_n,1);
ang = Dat(:,1);
D = Dat(:,2);
i = 1;
while i<=len_n
Fit = 100*exp(-1./(cos(ang*pi/180).^3*n(i,1)));
error(i,1) = sum(abs(Fit-D));
i = i+1;
end
tab = [n,error];
[m, p] = min(error);
best_n = tab(p)

fang = [ang(1,1):1:ang(end,1)];
Fitted = 100*exp(-1./(best_n*cos(fang*pi/180).^3));
figure
plot(ang,D,'*r',fang,Fitted)
title('Canopy Obscuration As A Function of Zenith Angle')
xlabel('Zenith Angle (degrees)')
ylabel('Percent Area Available for Laser Comms.')
```

```
figure
plot(n, error)
xlabel('n, best-fit parameter')
ylabel('Absolute Error')
title('n vs. Absolute Error')
```

Simulation Of FSO System Performance

Flyover1.m simulates an air-to-ground FSO link communicating through foliage. The UAV begins as a certain distance away from the receiver and the signal-to-noise ratio is determined as a function of the fractional unobscured area as well as the a basic noise calculation.

```
% Script file to test flyby
clc
close all
UAV.Altitude    = 2000;  % m
UAV.Velocity    =  100;  % m/s
GEOM.OffSet     =  0;  % m
GEOM.Start      =-5000;  % m
GEOM.Stop       = 5000;  % m
GEOM.Delta      =   100;  % m
XMIT.Power      =    2;  % W
XMIT.Beamwidth  =   60;  % Degrees
XMIT.WaveLength =  1.5;  % um
XMIT.Bandwidth  =   1;  % GHz
CANOPY.Height   =   20;  % m
CANOPY.LeafArea =   16;  % cm^2
CANOPY.LAI      =    2;  % Unitless
RCVR.Diameter   =   10;  % cm
DISPLAY.Ymin    =   -10; % dB
DISPLAY.Ymax    =   30; % dB
FlyOver1(UAV, GEOM, XMIT, CANOPY, RCVR,DISPLAY)
```

```
function flyover1(UAV,GEOM,XMIT,CANOPY,RCVR,DISPLAY)
% flyover1(UAV,GEOM,XMIT,CANOPY,RCVR,DISPLAY)
%
%
% = = = = = = = = = = = = = = = = = = = = = = = = = = = = = = = = =
% FILENAME:       flyover1.m                              %
% AUTHOR:         Clinton Edwards, University of Maryland      %
% DATE:           30 June 2004                            %
% = = = = = = = = = = = = = = = = = = = = = = = = = = = = = = = = =%
% UAV.            Structure defining UAV parameters           %
%    Altitude:    UAV altitude (m)                         %
%    Velocity:    UAV velocity (m/s)                        %
% - - - - - - - - - - - - - - - - - - - - - - - - - - - - - - - -%
```

```
% GEOM.           Geometry of flYby                        %
%     OffSet:    Horizontal offset distance  (m)           %
%     Start:     Along track starting position (m)         %
%     Stop:      Along track stoping position (m)          %
%     Delta:     Incremental distance along track (m)      %
% - - - - - - - - - - - - - - - - - - - - - - - - - - - - -%
% XMIT.           Laser Transmitting System                %
%     Power:     Laser Power (W)                          %
%     Beamwidth:  Beamwdith (Degrees)                     %
%     WaveLength: Laser wavelength (um)                   %
%     Bandwidth:  Bandwidth (GHz)                         %
% - - - - - - - - - - - - - - - - - - - - - - - - - - - - -%
% CANOPY.         Forest canopy                           %
%     Height:    Canopy height (m)                        %
%     LeafArea:   Mean leaf area (cm^2)                   %
%     LAI:       Leaf Area Index (unitless)               %
% - - - - - - - - - - - - - - - - - - - - - - - - - - - - -%
% RCVR.           Receiving System                        %
%     Diameter:   Receiving aperture diameter (cm)        %
% - - - - - - - - - - - - - - - - - - - - - - - - - - - - -%
% DISPLAY         Y limits of SNR plot                    %
%     Ymin       Minimum Y axis value (dB)                %
%     Ymax       Maximum Y axis value (dB)                %
% = = = = = = = = = = = = = = = = = = = = = = = = = = = = =

Z       = UAV.Altitude;
V       = UAV.Velocity;
Y       = GEOM.OffSet;
X1      = GEOM.Start;
X2      = GEOM.Stop;
Delta   = GEOM.Delta;
Pt      = XMIT.Power;
Bmwdth  = XMIT.Beamwidth;
lambda  = XMIT.WaveLength;
Bndwd   = XMIT.Bandwidth;
Zc      = CANOPY.Height;
A       = CANOPY.LeafArea;
LAI     = CANOPY.LAI;
Dr      = RCVR.Diameter;
Ymin    = DISPLAY.Ymin;
Ymax    = DISPLAY.Ymax;

Theta = Bmwdth/2;              % Beam half-angle
A=A/1e4;                    % Convert A to m^2
Dr=Dr/1e2;                  % Convert Dr to m
```

```
Lf=sqrt(A);                 % Mean leaf length
Ls=sqrt(pi)*Dr/2;             % Equivalent square length
n=ceil(Ls/Lf)               % n^2 = number of cells in aperture

Xa    =  [X1:Delta:X2];
Ra    =  sqrt(Xa.^2+Y^2+Z^2);    % Range array
L     =  zeros(size(Xa));       % Initialize SNR array
Phi   =  zeros(size(Xa));       % Initialize depression angles
matrix = rand(n,n);
Accum=0;                    % Initialize Accum
for m=1: length(Xa)
  X     = Xa(m);
  R     = Ra(m);              % Theta=acos(Z/R);
  eLAI  = LAI*R/Z;            % LAI./cos(Phi)

  Phi(m) = acos(Z/R)*180/pi;    % Depression Angle
  Thresh = 1-exp(-eLAI);
  Frac   = length(find(matrix>Thresh))/n^2;
%   Beam   = Phi(m)<Theta;        % 1 inside of beam o.w. zero
  Beam=1;
  Frac_Beam   = max(Frac*Beam,1e-6);      % Insures Frac > 0
  L(m)   = 10*log10(Frac_Beam);      % Propagation loss in dB

                        % Next Xa position in terms of cells

  if n*Lf<=Delta                  % No aperture overlab for next Xa position
     matrix=rand(n,n);
  elseif n*Lf<=Delta+Ls
    s=floor((n*Lf-Delta)/Lf);     % overlapping cells
    matrix=[matrix(:,n-s+1:n),rand(n,n-s)];
  else
     Accum=Accum+Delta;
     if Accum>=Lf
        matrix(:,1)=[];
        matrix=[matrix,rand(n,1)];
        Accum=0;
     end
  end

end

Out = SNR(Pt,Theta,Ra,Bndwd,lambda,L,Dr);
T=Xa/V;       %Time

figure
```

```
plot(T,Out)
xlabel('Time (sec)')
ylabel('SNR (dB)')
A=axis;
A(3)=Ymin;
A(4)=Ymax;
axis(A);
% Phidata=Phi
figure
plot(T, Phi)
ylabel('zenith angle (deg)')
xlabel('Time (sec)')



function Out=SNR(Pt,Theta,R,BW,lambda,L,Dr)
% function Out=SNR(Pt,Theta,R,BW,lambda,L,Dr)
%-------------------------------------------%
% O      = Receive SNR in dB                %
% Pt     = Trnsmit Power in Watts           %
% Theta  = Half angle beam in degrees       %
% R      = Range in meters                  %
% BW     = bandwidths in GHz                %
% lambda = wavelength in um                 %
% L      = Prop Loss or Transmittance in dB %
% Dr     = Rcvr Aperture Diameter in meters %
%-------------------------------------------%
% convert to meters
lambda=lambda*1e-6;
%convert L to unitless ratio
L=10.^(L/10);
% Transmit beam directivity
F=2/(1-cos(Theta*pi/180));
% Receive Power density (W/m^2)
p=Pt*F./(4*pi*R.^2);
p=p.*L;
% Receive Power (W)
Pr = p*pi*(Dr/2)^2;

% Thermal Noise
c=3e8; %m/s
F=c/lambda;
TN=ThermalNoise(F,290);
%Quantum Noise
```

```
QN=QuantumNoise(F);
% Total Noise
N=TN+QN;
% Convert BW to Hz
BW=BW*1e9;
%Total Noise
Nt=N*BW;

Out=10*log10(Pr/Nt);

%From W. Alan Davis, Microwave Semiconductor Circuit Design, p. 172
function N=ThermalNoise(F,T)
%function N=ThermalNoise(F,T)
%-------------------------
% N is in units of Watts/Hz
% F is in units of Hz
% T is in units of Kelvin
%-------------------------

%Planck's constant
h=6.6254e-34;  %Joule-sec
%Boltzman's constant
k=1.38049e-23;  %Joule/K
N=h*F./(exp(h*F/(k*T))-1);

function N=QuantumNoise(F)
%function N=QuantumNoise(F)
%-------------------------
% N is in units of Watts/Hz
% F is in units of Hz
%-------------------------
%Planck's constant
h=6.6254e-34;  %Joule-sec

N=.5*h*F;
```

Bibliography

[1] C. C. Davis. *Lasers and Electro-Optics*. Cambridge University Press, 1996.

[2] J.G. Fleischman, S. Ayasli, E. M. Adams, and D. R. Gosselin. *Part 1: Foliage Attenuation and Backscatter Analysis of SAR Imagery.* IEEE Transactions on Aerospace and Electronics Systems Vol. 32 135—144, January 1996

[3] I. I. Kim, B. McArthur, and E. Korevaar. *Comparsion of Laser Beam Propagation at 785nm in Fog and Haze for Optical Wireless Communications.* (http://www.opticalaccess.com)

[4] R. A. Shaw, A B. Kostinski, and D. D. Lanterman, *Super-Exponential Extinction of Radiation in a Negatively-Correlated Random Medium,* Elsevier Science, August 2001

[5] *Introduction to Beer's Law,* (http://www.shu.ac.uk/schools/sci/chem/tutorials/molspec/beers1.htm)

[6] J. M. Vose, N. H. Sullivan, B. D. Clinton, and P. V. Bolstad, *Vertical Leaf Area Distribution, Light Transmittance, and Application of the Beer-Lambert Law in Four Mature Hardwood Stands in the Southern Appalachians,* Canadian Journal of Forest Reserves, Vol. 25, 1036—1043, 1995

[7] Beer-Lambert Law (http://elchem.kaist.ac.kr/vt/chem-ed/spec/beerslaw.htm)

[8] H. Chen, Z. Wu, R. Yang, and L. Bai, *Gaussian Beam Scattering From Arbitrarily Shaped Objects With Rough Surfaces,* Institute of Physics Publishing: Waves in Random Media, Vol. 14 277—286, 2004

[9] A. D. Vecchia, P. Ferrazzoli, and L. Guerriero, *Modeling Microwave Scattering From Long Curved Leaves*, Institute of Physics Publishing: Waves in Random Media, Vol. 14 S333—S343, 2003

[10] M. Achour, *Free-Space Optics Wavelength Selection: 10um Versus Shorter Wavelength*, Optical Society of America: Journal of Optical Networking, Vol. 2 127—143 , June 2003

[11] D. V. Hahn, C. L. Edwards, D. D. Duncan, *Link Availability Model for Optical Communication through Clouds,* SPIE Conference Proceedings 4821—4837, 2002

[12] LIDAR/SLICER (http://www.eoc.csiro.au/lidar/slicer/slicer.htm)

[13] SLICER flight paths: SERC (http://denali.gsfc.nasa.gov/lapf/slicer/95serc/95serc.html)

[14] SLICER Laser Altimeter Processing Facility (http://denali.gsfc.nasa.gov/lapf/)

[15] Lidar Remote Sensing of Forest Structure (http://www.fsl.orst.edu/~lefsky/slicerpage.html)

[16] R. O. Dubayah, and J. B. Drake, *Lidar Remote Sensing for Forestry Applications,* Journal of Forestry, Vol. 98 44—46, 2000

[17] Modeling Leaf Optical Properties (http://www.sigu7.jussieu.fr/Led/LED_leafmod_e.htm)

[18] S. N. Martens, S. L. Ustin, and J. M. Norman, *Measurement of Tree Canopy Architecture,* International Journal of Remote Sensing Vol. 12 1525-1545, 1991

[19] S. N. Martens, S. L. Ustin, R. A. Rousseau, *Estimation of Tree Canopy Leaf Area Index by Gap Fraction Analysis,* Forest Ecology and Management (in press) 1993

[20] H. Fang, and S. Liang, *Retrieving Leaf Area Index with a Neural Network Method: Simulation and Validation,* IEEE Transactions on Geoscience and Remote Sensing, Vol. 41 2052—2062, September 2003

[21] W. Ni-Meister, D. L. B. Jupp, R. Dubayah, *Modeling Lidar Waveforms in Heterogeneous and Discrete Canopies,* IEEE Transactions on Geoscience and Remote Sensing, Vol. 39 1943—1958, 2001

[22] C. C. Davis and I. I. Smolyaninov. *The Effect of Atmospheric Turbulence on Bit-Error-Rate in an On-Off-Keyed Optical Wireless System,* SPIE Conference Proceedings: Free-Space Laser Communication and Laser Imaging, 126—137, 2001